Evaluation and Application of Thermal Modeling for High Power Motor Improvements

Ethan L. Filip

Thesis submitted to the faculty of the Virginia Polytechnic Institute and State University
in partial fulfillment of the requirements for the degree of

Master of Science
In
Mechanical Engineering

Douglas J. Nelson – Chair
Michael W. Ellis
John B. Ferris

November 12, 2010
Blacksburg, VA

Keywords: Nodal Thermal Model, Electric Vehicle Motor, Thermal Conductivity

Evaluation and Application of Thermal Modeling for High Power Motor Improvements

Ethan L. Filip

ABSTRACT

Electric motors for vehicle applications are required to have high efficiency and small size and weight. Accurately modeling the thermal properties of an electric motor is critical to properly sizing the motor. Improving the cooling of the motor windings allows for a more efficient and power-dense motor. There are a variety of methods for predicting motor temperatures, however this paper discusses the advantages and accuracy of using a nodal lumped thermal model. Both commercially available and proprietary motor thermal modeling software are evaluated and compared. Thermal improvements based on the model in both contact interfaces and winding encapsulant are evaluated, showing motor improvements in the ability to handle heat losses of approximately forty percent greater than the baseline, resulting in either higher power or lower motor temperatures for the same package size.

Table of Contents:

List of Multimedia Objects:

Figures

Tables

Equations

1.0 Introduction

1.1 Problem

Electric vehicle motors are required to be lightweight, and very power-dense in order to be packaged within the given space and to allow a vehicle to meet performance specifications. Electric vehicle motors are typically sized based upon thermal limitations, as decreasing the package size limits the available motor area for cooling. The thermal loading is due to I^2R losses in motor copper, as well as eddy current losses within the steel and magnets of a motor. This paper focuses on motors in the range of 200 – 300 kW for vehicle applications. These motors are liquid-cooled in order to meet performance targets while operating in an under-hood environment with temperatures exceeding 100 °C. The motor liquid cooling is on a lower temperature circuit than the engine, with coolant temperature in the range of 75-85 °C. This paper focuses on modeling and improvements to thermal performance of high power vehicle motors, and therefore improvements to the overall motor performance given the challenging under-hood environment.

1.2 Objectives

The purpose of this paper is to evaluate and test improvements in the cooling performance of high-power vehicle motors. Improved cooling is achieved through evaluating, tuning and verifying motor thermal models, and then using those models to identify, build and test significant thermal improvements.

The thermal modeling methods for liquid-cooled motors are evaluated, with a comparison between two separate thermal models that are tuned with tested motor thermal performance. Correlation and tuning of existing thermal models is required due to the unique thermal pathway of high power liquid-cooled motors vs. the conventional air-cooled motors that these models were originally based upon and correlated to. Thermal performance is measured by the magnitude of losses that a motor can withstand without exceeding a peak winding temperature of 200°C. The higher magnitude of motor thermal losses withstood represents a thermal improvement, and ultimately results in higher motor power output without increasing the motor package size or weight.

The tuned and verified thermal models are utilized to obtain a focused path for improved thermal performance. This improved motor is then built and thermally tested to compare the model-predicted thermal performance to the actual test values, verifying the improvements.

1.3 Discussion

The ability to accurately model the thermal performance of a high-power liquid-cooled motor is critical in both the quotation and design stages of motor development. Thermal performance estimates are needed in order to ensure that the motor will fit within the allotted space and meet the required performance and efficiency criteria. Motors of this size and power range are very expensive to prototype, and it is not practical to build motors for each new design in order to verify thermal assumptions. Cross sections of liquid cooled motor models are shown in Figure 1 and Figure 2.

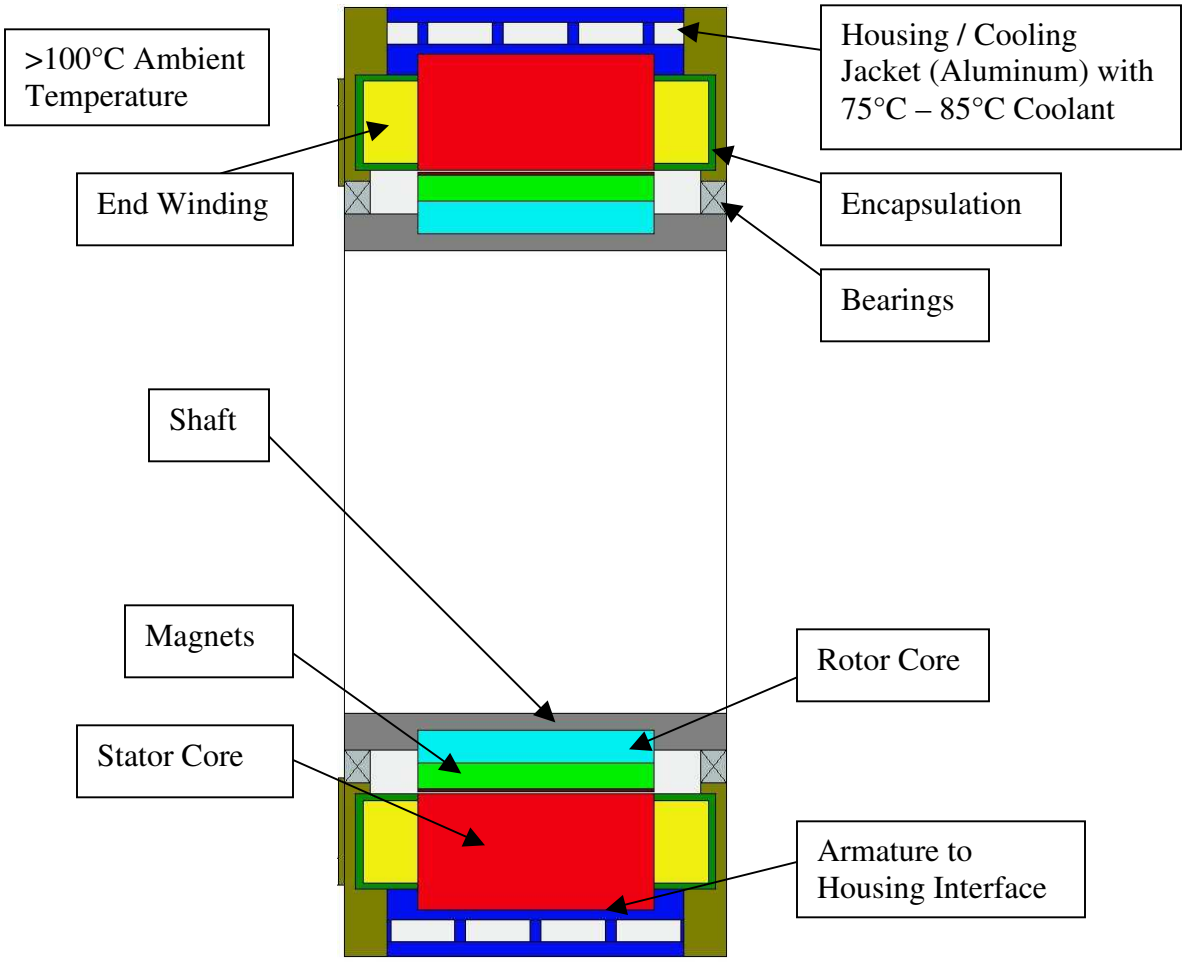

Figure 1 – Motor Axial Cross Section

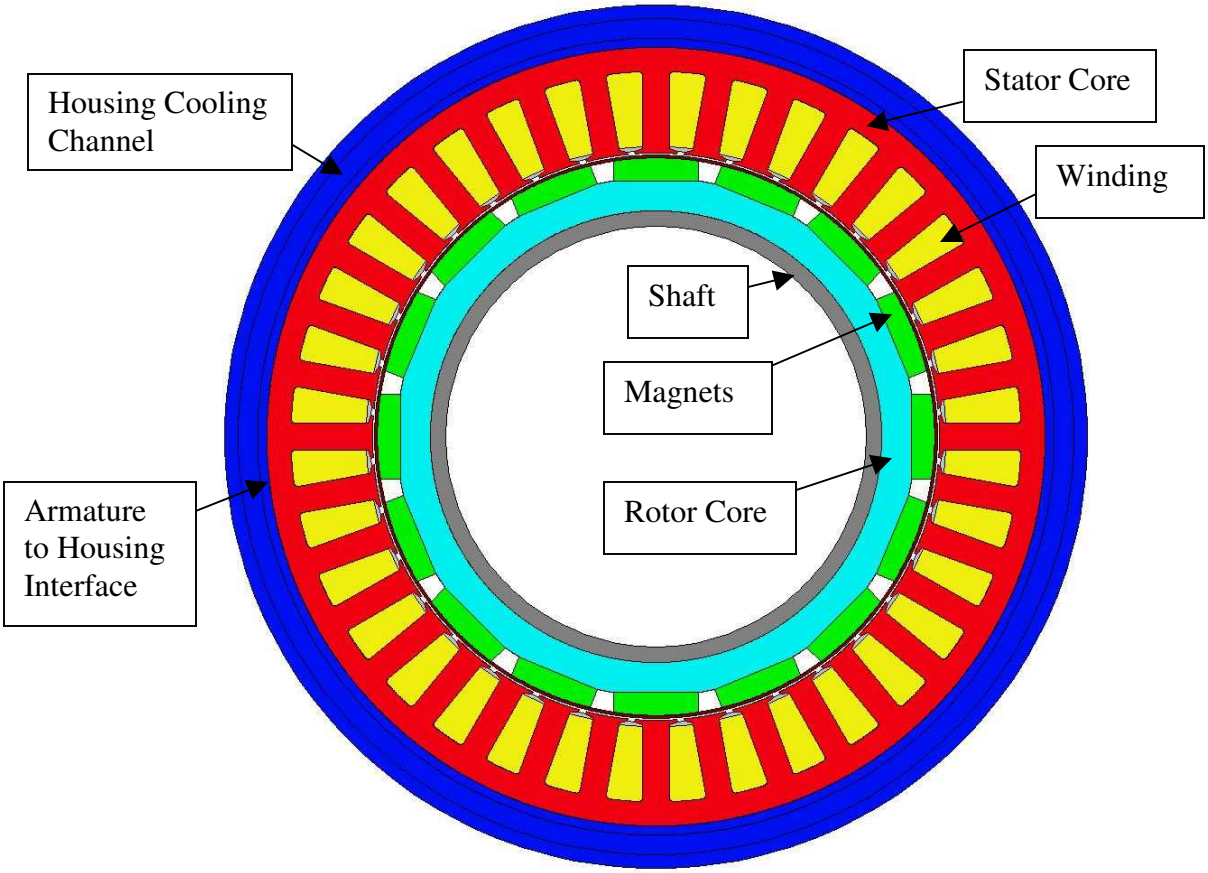

Figure 2 – Motor Radial Cross Section

One thermal improvement parameter that has a large impact on motor performance is the thermal conductivity of the winding encapsulant. Winding encapsulation is an electrical insulator used to retain copper windings within a motor core, and also improve the thermal pathway between the copper and the liquid cooled motor core. This winding encapsulation change is the focus of this paper, as a 39% motor performance improvement was achieved through improvements in the motor winding encapsulation, as shown in Section 5.0, Results Summary. The ability to quantify thermal improvement in the motor design is important, as the improved encapsulant adds cost to the motor in both material costs and manufacturing time. With

an accurate thermal model, these costs can be justified by illustrating the increased motor power or decreased motor packaging that can be achieved.

Other thermal improvement areas that have been considered but are not covered in-depth in this research include gaps and voids within the motor. The gap between the armature and housing is shown to have a very large effect on high-power, water-cooled motors, however this is difficult to change and measure within a motor. This joint is typically optimized for structure while minimizing thermal resistance. Voids within the high voltage slot liner system and air bubbles within the encapsulant are also present within high-powered motors, however this is challenging to quantify without complete destruction of the motor, and it does not show up in the thermal models evaluated. Improvements in the encapsulation system include process changes in order to minimize void formation.

2.0 Literature Review

2.1 Thermal Modeling approach

Evolution and Modern Approaches for Thermal Analysis of Electrical Machines [1]

This paper provides some input as to the best tools and practices available for motor thermal modeling. The paper may have some bias towards nodal models, as one of the authors started the company that produces Motor-CAD™ [2], a commercially available nodal thermal model for motor analysis. Motor-CAD™ is also utilized in this thesis as one of two nodal thermal models analyzed. Finite Element Analysis (FEA), Computational Fluid Dynamics (CFD), and Lumped–Circuit Modeling (nodal) are discussed. The importance of thermal modeling and limitations are also discussed.

FEA modeling is discussed as useful for motors that are not of a standard type having irregular geometry. This method of analysis is described as very time-consuming to set up, as well as time-consuming to run. FEA has the advantage over a lumped parameter model with the ability to locate motor hot spots that may not be located at the exact placement of the lumped parameter node, however a well-defined network is much more practical to run.

The advantage of CFD analysis is illustrated in the ability to improve sections of a motor, such as airflow or coolant flow, however the current primary function of CFD is not as a tool to evaluate the full motor thermal properties. The authors discuss that CFD analysis coupled with a lumped parameter network is the best way to utilize CFD.

Lumped parameter modeling is discussed as a fast analytical network based upon simplified geometry to develop a circuit of thermal resistances. The lumped parameter thermal network typically requires a standard motor geometry and the thermal circuit

must include the "main heat transfer paths". The lumped parameter thermal network model is shown to be limited by knowledge of the thermal parameters and heat transfer coefficients, however this limitation is accurately stated to also apply to numerical modeling approaches such as FEA.

Although critical parameters and interfaces are discussed only briefly in the conclusions of this paper, three of the authors contributed to *Determination of Critical Parameters in Electrical Machine Thermal Models*[3], a more thorough review, and [4] a very similar paper.

2.2 Critical Parameters

Determination of critical parameters in electrical machine thermal models.[3]

The main theme of this paper is a discussion of the critical parameters that must be determined in order to have an accurate motor thermal model, regardless of modeling technique. The paper focuses on seven parameters:

1. *Equivalent Thermal Resistance Between Frame and Ambient and Zero Fan Speed*
2. *Equivalent Thermal Conductivity Between Winding and Lamination*
3. *Forced Convection Heat Transfer Coefficient Between End Winding and End-Caps*
4. *Radiation Head Transfer Coefficient Between External Frame and Ambient*
5. *Interface Gap Between Lamination and External Frame*
6. *Air Cooling Speed*
7. *Bearing Equivalent Thermal Resistance*

While these parameters help illustrate the difficulties in setting up an accurate thermal model, they are mostly related to air-cooled models. For water-cooled, encapsulated

motors, such as those used in high-power vehicle applications, only two of these critical parameters are relevant - *Equivalent Thermal Conductivity Between Winding and Lamination* and *Interface Gap Between Lamination and External Frame.*

The thermal conductivity between the windings and lamination is shown to be approximated using three different methods. One of the models is based upon a fit curve correlation with existing measurements, another model is a 2D FEA of windings simulated at an even spacing, and the third is a layered winding model with equivalent resistances. The commercial software uses the winding model for the ease of inputs and customization. The model utilizes material properties, combined with an impregnation "goodness" factor to account for air or voids within the motor winding impregnation.

The lamination to frame interface gap is discussed as necessary to accurately determine the thermal resistance to the frame. Examples of thermally measured interface gaps are shown to be variable throughout a range of motor sizes, ranging from 0.01 mm to 0.08 mm. This range is shown to have a significant effect on motor cooling. The authors also noted that identical motor designs have been measured to have differences in interface gaps. This value is later shown to be especially critical in liquid-cooled motors, where the thermal pathway is through this interface to the cooling liquid.

The paper "Solving the More Difficult Aspects of Electric Motor Thermal Analysis" [4] is by the same authors as [3], and looks and many of the same parameters. An addition in [4] is the inclusion of a discussion of thermal transfer across a motor air-gap. The air-gap discussion includes the increase in heat transfer when the rotor or stator diameter is not smooth, however this feature is not critical to high-powered vehicle motors.

2.3 Thermal Networks

The paper Lumped parameter thermal model for electrical machines of TEFC *(Totally Enclosed, Fan Cooled)* design [5] by Mellor is the basis for many additional papers on the conventional lumped parameter thermal model, including specific papers for permanent magnet motors and water cooled motors [6]. An additional example is the interior permanent magnet model by Ayman [7]. This conventional model is the basis of both the internally developed and commercially available software used in this paper.

Improvements to the conventional lumped parameter thermal model have been proposed in multiple papers by Gerling. The paper Novel lumped-parameter thermal model for electrical systems [8] discusses a model in which a solid element is considered instead of just a node, allowing for the distribution of losses and temperature within the element. Model improvements also include moving nodes in order to hit the peak temperature points for the node location. This method does address the conventional thermal model concern of nodes representing average temperatures, while for some motor materials it is important only to know the peak temperatures.

The paper An Improved Lumped Parameter Thermal Model for Electrical Machines [9] offers a good summary of the importance in obtaining an accurate thermal model, allowing for properly sizing the motor and ensuring materials will withstand the environment. The paper also discusses sensitivity arising from the stator-to-housing gap, and slot liner material properties, but it does not offer a good modeling solution for either of those issues other than to recommend testing. The paper also discusses compensation elements, similar to [8] and the improvements made to the thermal model. The majority of the model differences are in the end-winding, copper, and teeth, where the thermal losses would be distributed throughout. The model is verified against an FEA thermal

model instead of actual part testing. Therefore, as a concept for a model the improvements have merit, however the model should be tested on real parts for confirmation.

The complexities in the model suggested by Gerling [8,9], while they do appear to be improvements, seem to offer limited benefit to simply distributing additional nodes within the teeth, copper, and end winding. The Motor-CAD™ commercial modeling software used in this paper already includes an array of distributed nodes for the copper. Future work could include adding nodes to the teeth and end windings to account for this distributed loss discrepancy.

3.0 Modeling

3.1 Lumped Parameter Modeling Benefits and Drawbacks for High Powered Motors

A lumped parameter model is a representation of a physical system at discrete points instead of a distribution of the entire system, such as an electrical circuit represented by discrete components such as resistors. Lumped parameter modeling is utilized for both the internally developed Thermsim software and the commercially available Motor-CAD™ [2] software due to the ease of simulation and modeling speed. This allows multiple iterations, with a calculation time that is completed within a few seconds for a steady state analysis and usually under one minute for a transient analysis, depending on the number of discrete transient condition points evaluated. Both software packages allow geometry inputs that provide a close representation to the motor being evaluated, typically allowing for an accurate representation. This speed allowed from a simplified model offers a great advantage over a finite element thermal model, especially as the deviations from actual to predicted values are rarely dependent on geometry discrepancies. Deviations from predicted values are mostly from unknown or hard-to-determine interface and material properties, which would affect a finite element solution in the same manner.

Lumped parameter modeling would not be the best modeling solution if the motor geometry is vastly different from an existing model. There are savings of both time and money realized by running a finite element solution versus setting up a new nodal network model. This is particularly true if there are no plans to re-use the new nodal network model for future analyses. The motor being analyzed for this vehicle application

fits existing permanent magnet brushless motor model geometry and it is therefore very effective to use the lumped parameter method.

One issue with the existing models is that the geometry does not change along with transient motor conditions. An example of this is the gap between the motor core and the housing. The importance of this parameter is shown in [3] referenced earlier and is also illustrated in the sensitivity analysis in Section 3.4. This gap is dependent upon the temperature difference between the housing and the core, and the aluminum housing and steel laminations have different coefficients of thermal expansion. With current software, the gap remains constant with changing temperatures. This requires manual iteration of the gap geometry in order accurately predict the motor temperature.

3.2 Thermsim

Thermsim is internally developed proprietary thermal modeling software. It is based upon the equations in Mellor's paper [4] with the thermal resistance network shown in Figure 3. The model is solved using Matlab™, with the setup and programming utilizing Simulink™ as shown in Figure 4. Microsoft Excel is utilized for inputs and outputs with the Simulink™ model, as well as for solving thermal resistance and thermal capacitance parameters. The inputs for Thermsim include the material properties and geometry for the housing, laminations, magnets, encapsulation, and windings, as well as the winding heat properties and the water cooling geometry and flow properties. Thermsim inputs sheets for are shown in Appendix A. An example of a resistance model is shown in Figure 5, while correlation factors are shown in Figure 6**.** Parameters passed to the Simulink™ model from Excel include thermal resistance, thermal capacitance,

motor speed, motor torque, loss information, and cooling fluid parameters. Simulink™ can also be utilized directly for outputs, as shown in Figure 7.

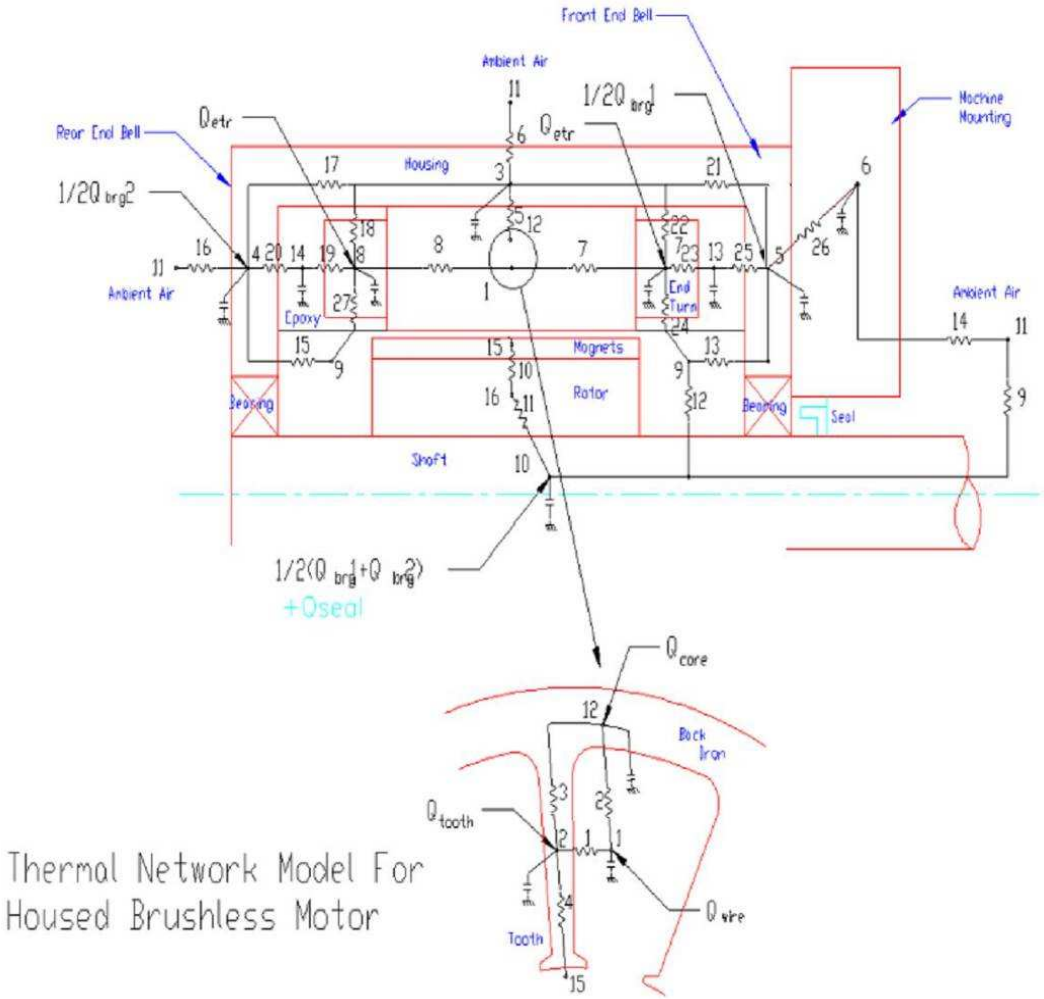

Figure 3 - Thermal Network Model

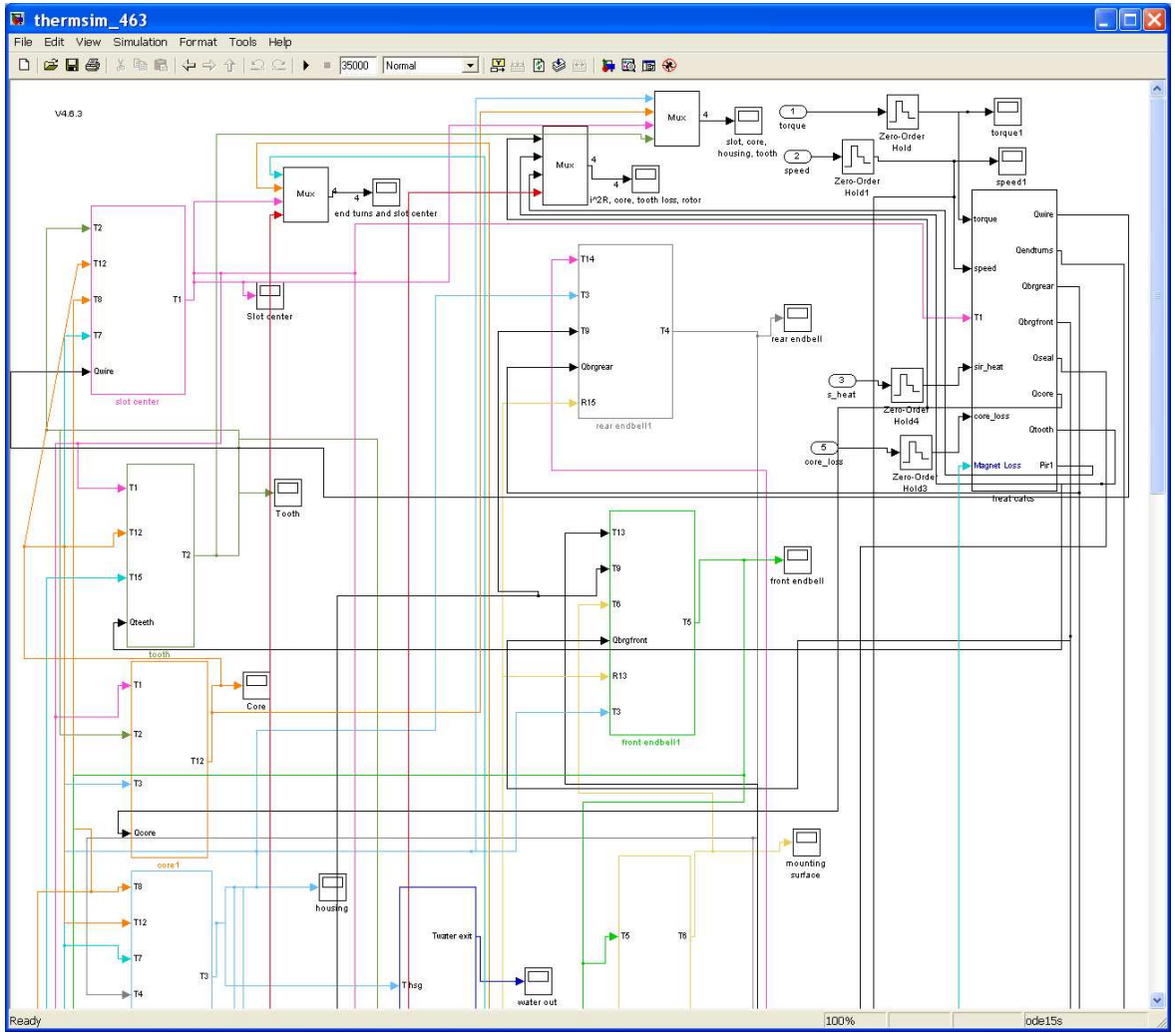

Figure 4 - Simulink Thermal Model Example

The benefits to utilizing this internally developed software include a history of correlation with a variety of production motors, as well as the ability to explore and understand the assumptions made for each thermal resistance and capacitance. Motor thermal testing is time-consuming and expensive; therefore this correlation to real motor testing is a valuable asset of this software. However a correlation study with the existing test data could easily be reproduced for new software given that the testing has already been completed. The ability to explore and edit the equations and assumptions made for each thermal resistance and capacitance is very valuable for obtaining an accurate correlation and interpreting results for a motor type that has any geometry or winding variations from the standard setup, as is often the case with high power vehicle motors. This openness facilitates troubleshooting any discrepancies between the tested values and model assumptions on an area or thermal resistor level.

Drawbacks to the internally developed software include the lack of visual results relative to motor geometry, the lack of visual inputs, the requirement of correlation factors as shown in Figure 6 and the limitation of motor type. The lack of visual outputs and inputs greatly reduces the ability to quickly recognize either input errors or calculation anomalies. Visual outputs also help illustrate areas of opportunity for improved cooling. For example, an output showing that the motor end-turns are very hot while the surround housing is cool, allows increased focus on the interface between the end-turns and windings providing significant benefits. The required use of correlation factors is due to model discrepancies versus actual geometry or when the actual geometry is not accurately known. Thermsim utilizes two correlation factors, a slot liner thermal resistance multiplier of 1.3 and a stator to housing gap multiplier of 2.0. These

correlation factors have been determined by adjusting to get a best fit of multiple tested thermal locations within a motor, including both end windings and slot top and bottom temperature measurements. The necessity of the correlation factors is likely due to voids in the encapsulation and unknown contact resistances in the slot and armature interface areas. Currently the internal software is only useful on brushless permanent magnet motors and induction motors. Significant re-programming would be required in order to utilize this tool for brush motors, outer rotor permanent magnet brushless motors, buried magnet PM motors, brushed motors and switched reluctance motors. Commercially available software was purchased and evaluated for these reasons.

R with air	**0.357534847**	
Rspace	0.003677126	endturn edge to space between endbell and endturn, axial
R20	**3.58E-01**	

Calculations:

ecap		
		radial direction, entire motor
r2	187.8932	
r1	145.6342	
Roa	0.011031378	
R1a	0.005515689	
Rma	-0.001838563	
Recap	0.003677126	
area convection	121640.7108	mm^2
Rair	5.28E-01	

Endbell, Length

Endbell Conduction

area	47,751	mm^2
length	3.81	mm
Rconduct - endbell	**4.78E-04**	deg C/W

Contact Drop

Estimated Gap	0.574	mm
conductivity of air	0.0000340	**W/mm/deg C**
area of ecap / housing interaface	47,751	mm^2
contact drop, slip fit	0.3534	**deg C / W**

Figure 5 - Thermal Resistance Calculation Example

Motor Components:	**Conductivity W/mm/deg C**	**Specific heat J/Kg/deg C**	**density Kg/m^3**	**reference:**
slot liner	0.000124615			correlation factor to match 1.30
housing	0.167	896	2700	
front endbell	0.167	896	2700	
rear endbell	0.167	896	2700	
shaft	0.052	465	7833	
mounting surface	0.167	896	2700	
laminations, radial	0.05096	465.000	7833	
magnet	0.167	460		
yoke	52	465	7833	
slot insulation	0.0026	1220	1828	
endturn insulation	0.0026	1090	1828	
interstitial stator / housing gap	1.34E-04			correlation factor to match 2.00
rotor coolant	0.000034	34	0.034	
rotor bars	0.167	896	2700	
Ecap to Alumimum Contact Drop		correlation factor to match test		

Figure 6 - Component Input Data with Correlation Factors

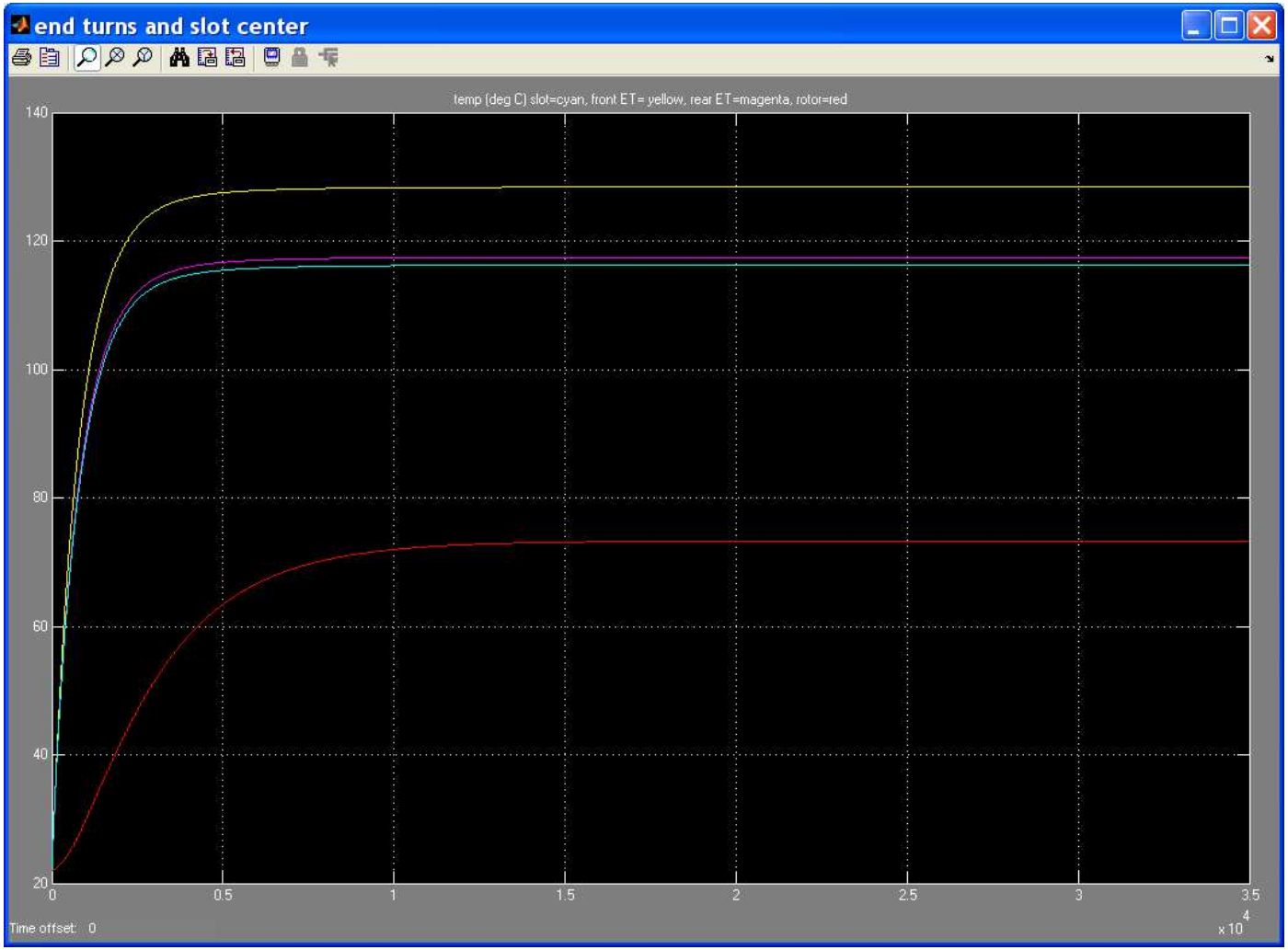

Figure 7 - Simulink Output Example

3.3 Motor-CAD™

The clearest benefit in using the commercially available Motor-CAD™ software is the graphical user interface. The software creates both axial and radial sections of the motor model as the geometry is input. This allows for a very clear and quick check to verify that the input geometry is accurate. Examples of these input pages are located in Figure 8 and Figure 9. Cooling and winding inputs are shown in Figure 10 and Figure 11, with the thermal network and circuit editor shown as Figure 12 and Figure 13. The output temperature results are displayed in a similarly clear manner, with temperatures displayed at nodes on the motor geometry. This view helps to illustrate where the hot spots and heat paths are located. This is illustrated in Figure 14 and Figure 15.

Motor-CAD™ inputs are very similar to Thermsim, consisting of known geometry and material properties for the housing, laminations, magnets, encapsulation, and windings, as well as the winding heat properties and fluid cooling geometry and flow properties. Motor-CAD™ also utilizes correlation factors, specifically impregnation goodness for the end winding, liner-lam interface, and active winding sections and potting goodness at the end winding. These correlation factors are available to account for unknown voids and contact resistance gaps present from the manufacturing process.

The nodal network for Motor-CAD™ is very similar to the nodal network for Thermsim, with a few additional features. The active winding is represented by a series of layers of encapsulant and copper, as opposed to the single point node in Thermsim. The nodal network also incorporates additional cooling pathways within the motor end-space, however this has little effect on a liquid cooled motor. The nodal network for Motor-CAD™ is flexible and changes based upon the cooling type selected.

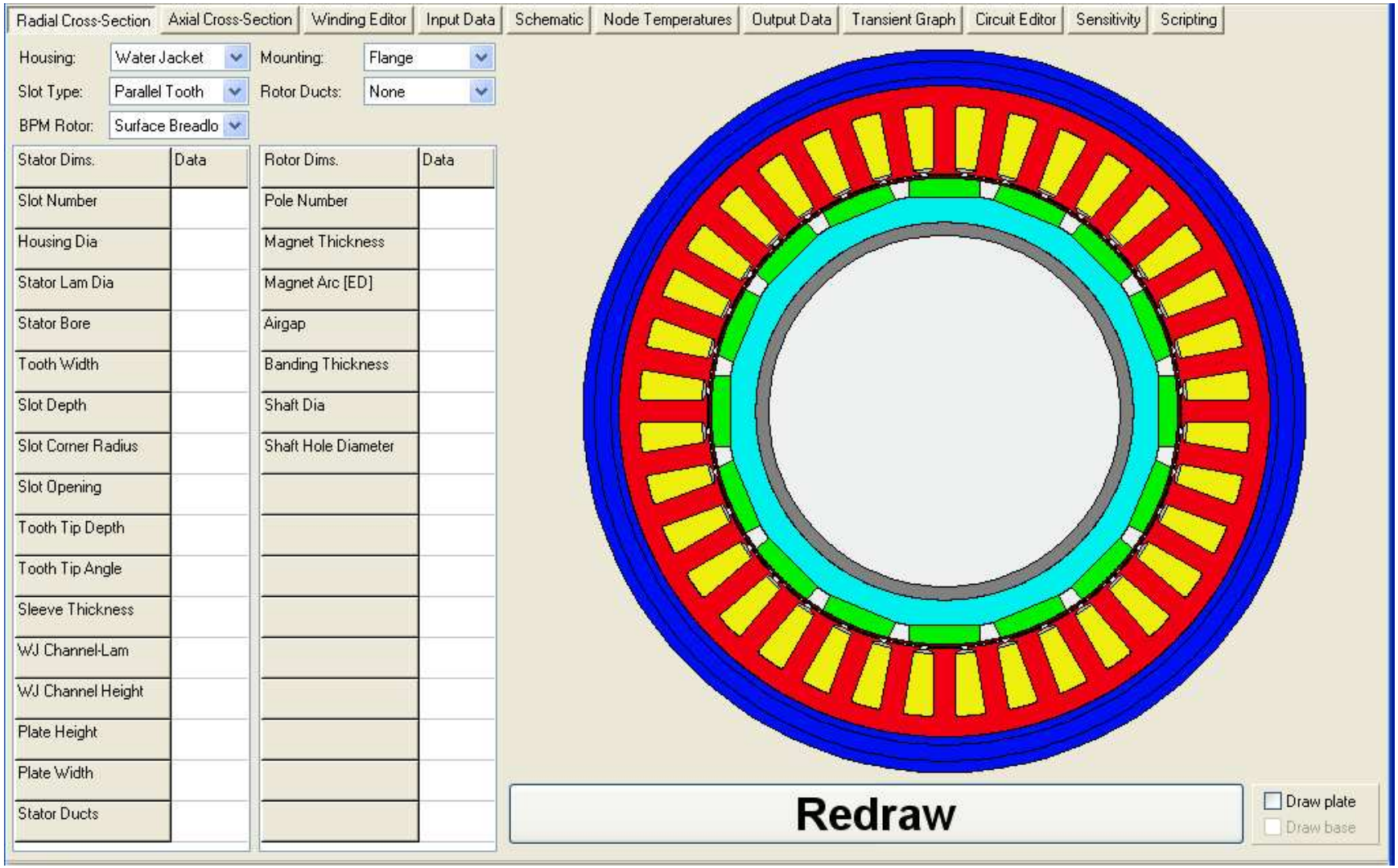

Figure 8 - Motor-CAD™ Input Sheet

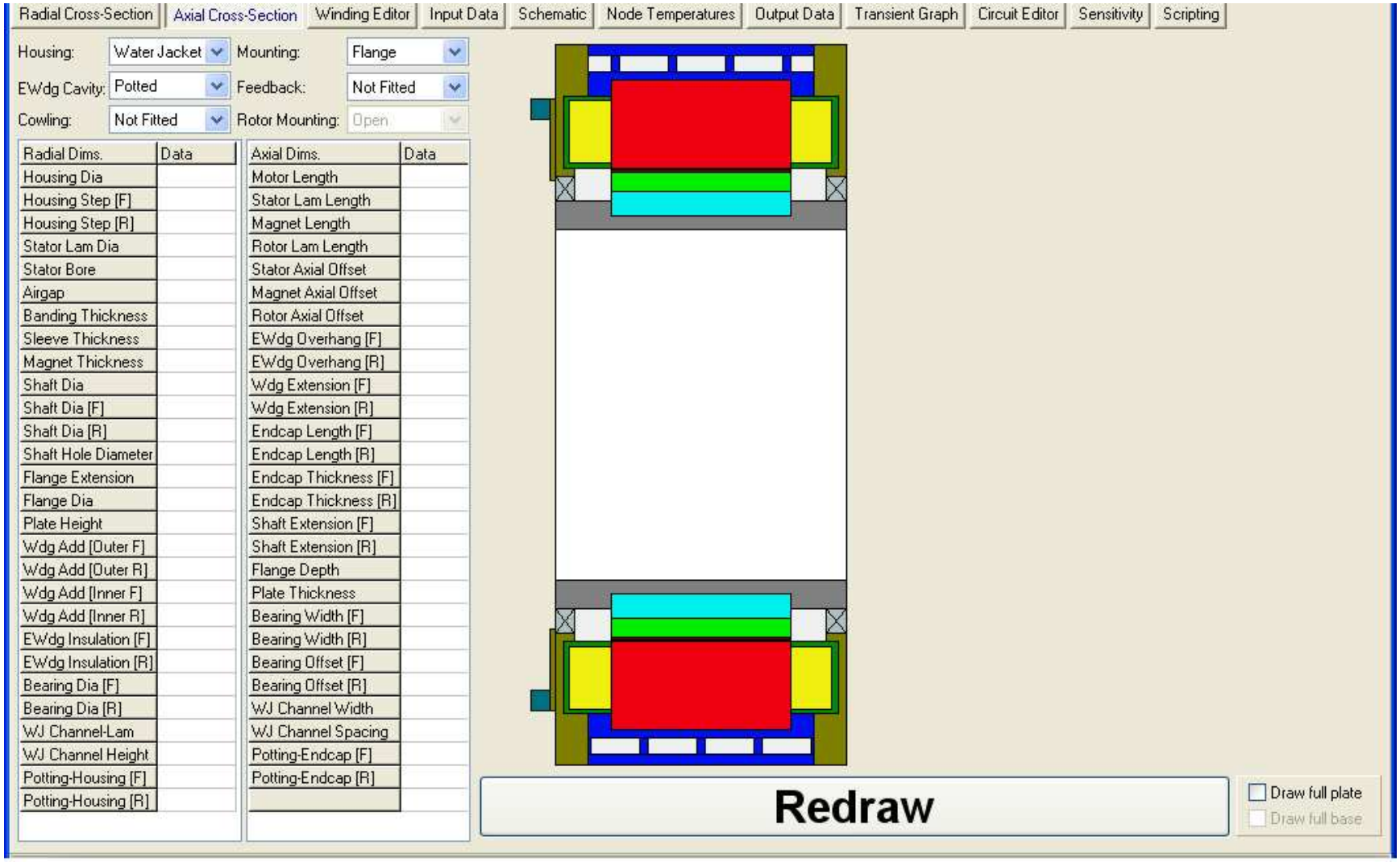

Figure 9 - Motor-CAD™ Input Sheet - Axial

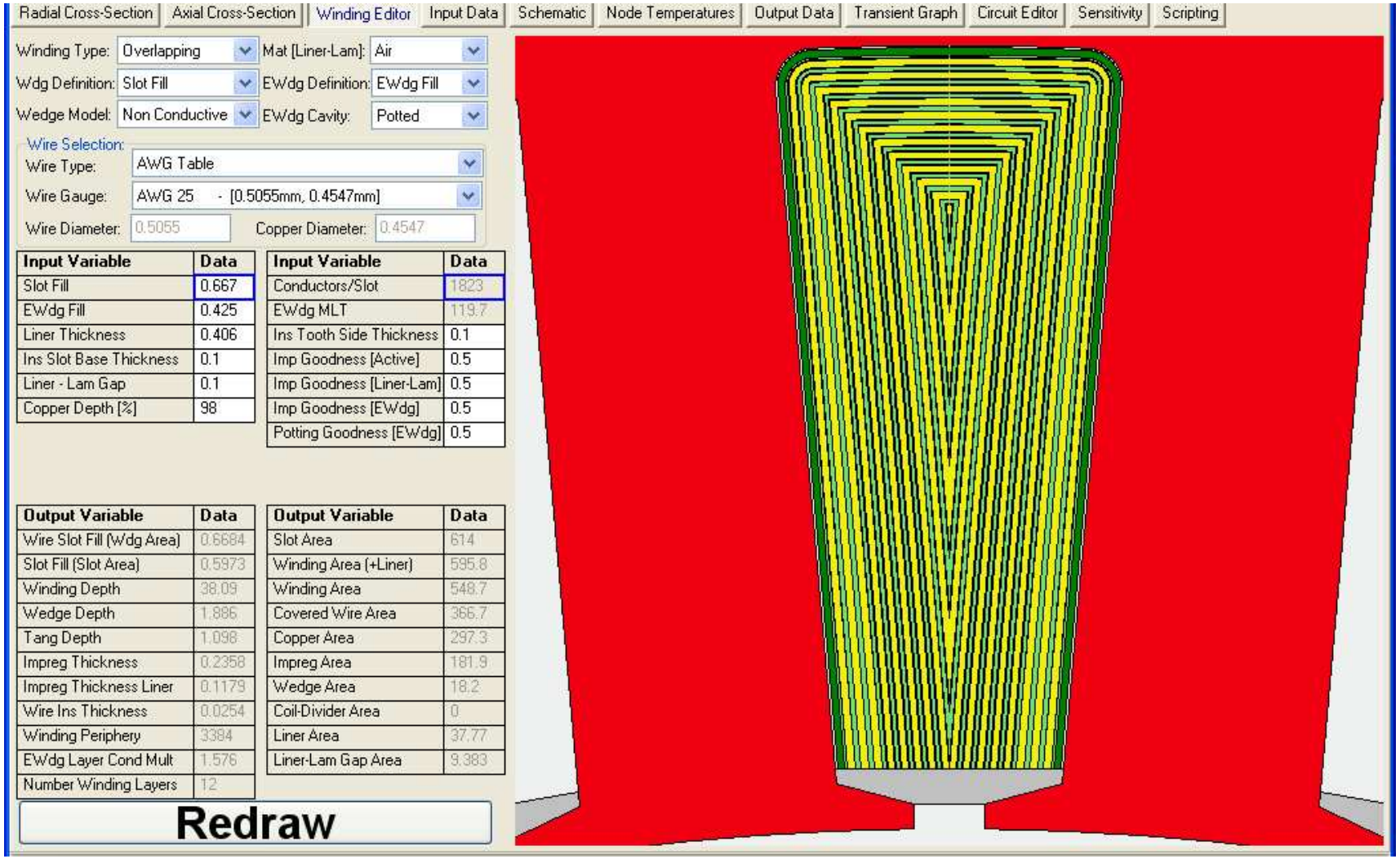

Figure 10 - Motor-CAD™ Input Sheet - Winding

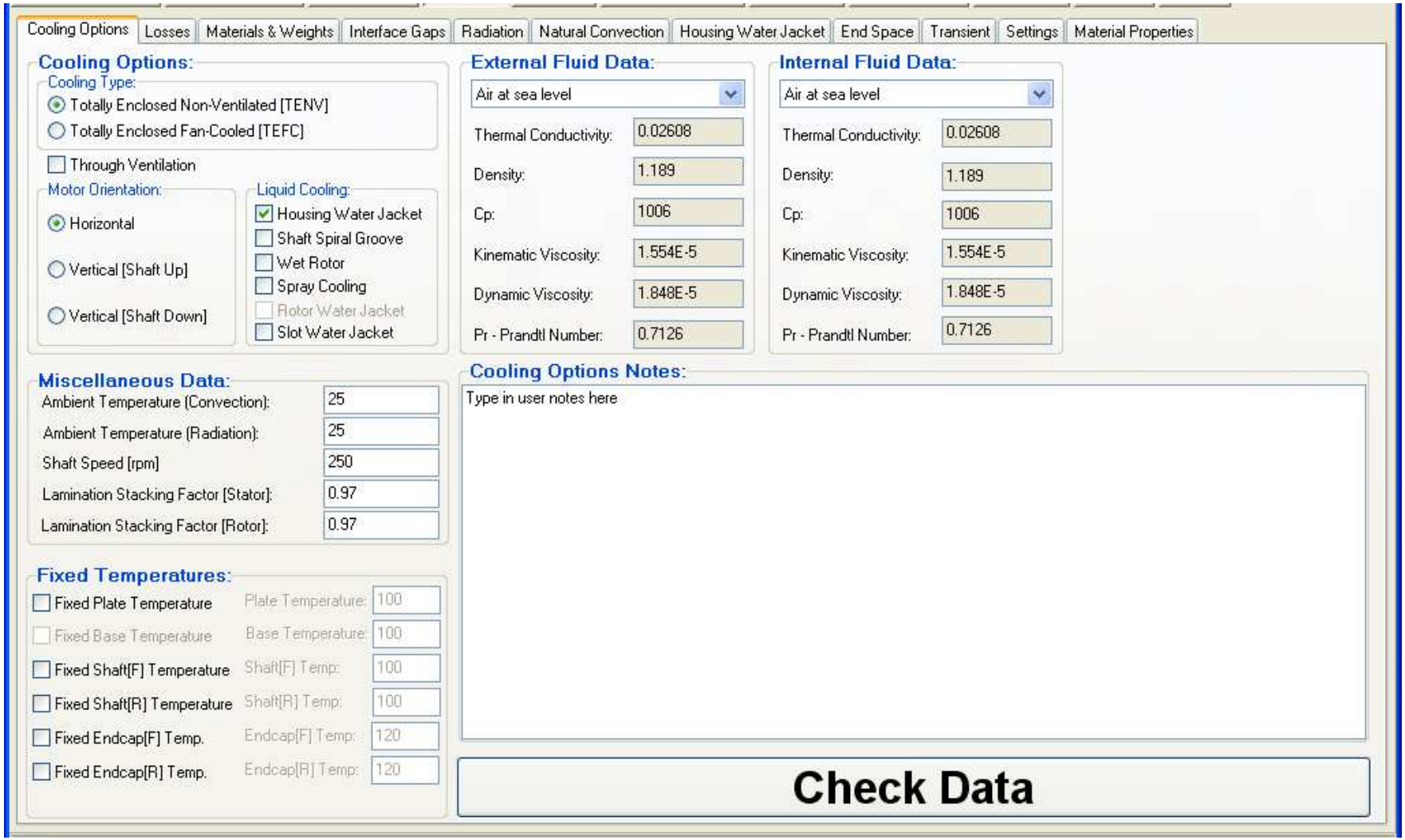

Figure 11 - Motor-CAD™ Input Sheet - Cooling

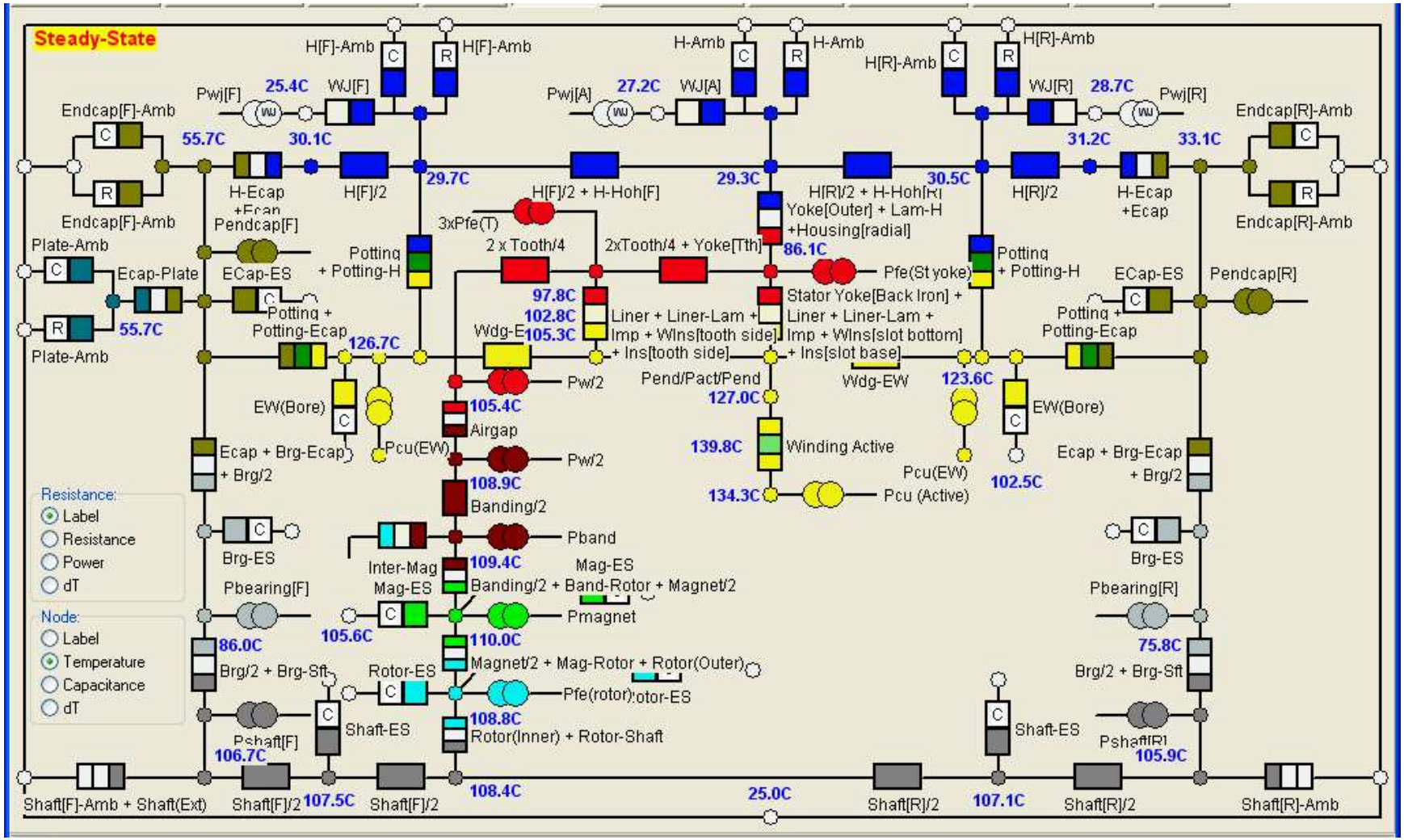

Figure 12 - Motor-CAD™ Nodal Network

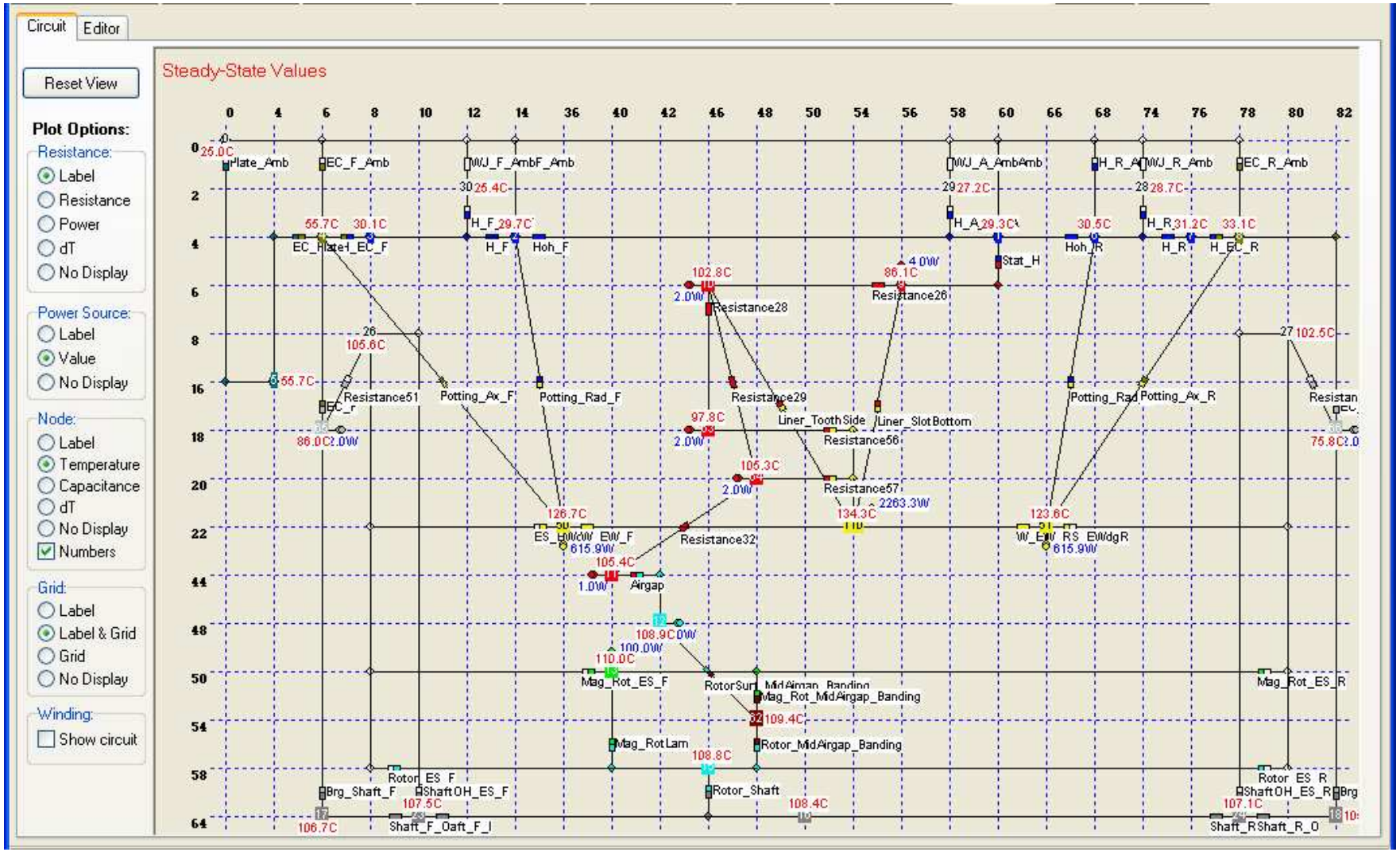

Figure 13 - Motor-CAD™ Circuit Editor

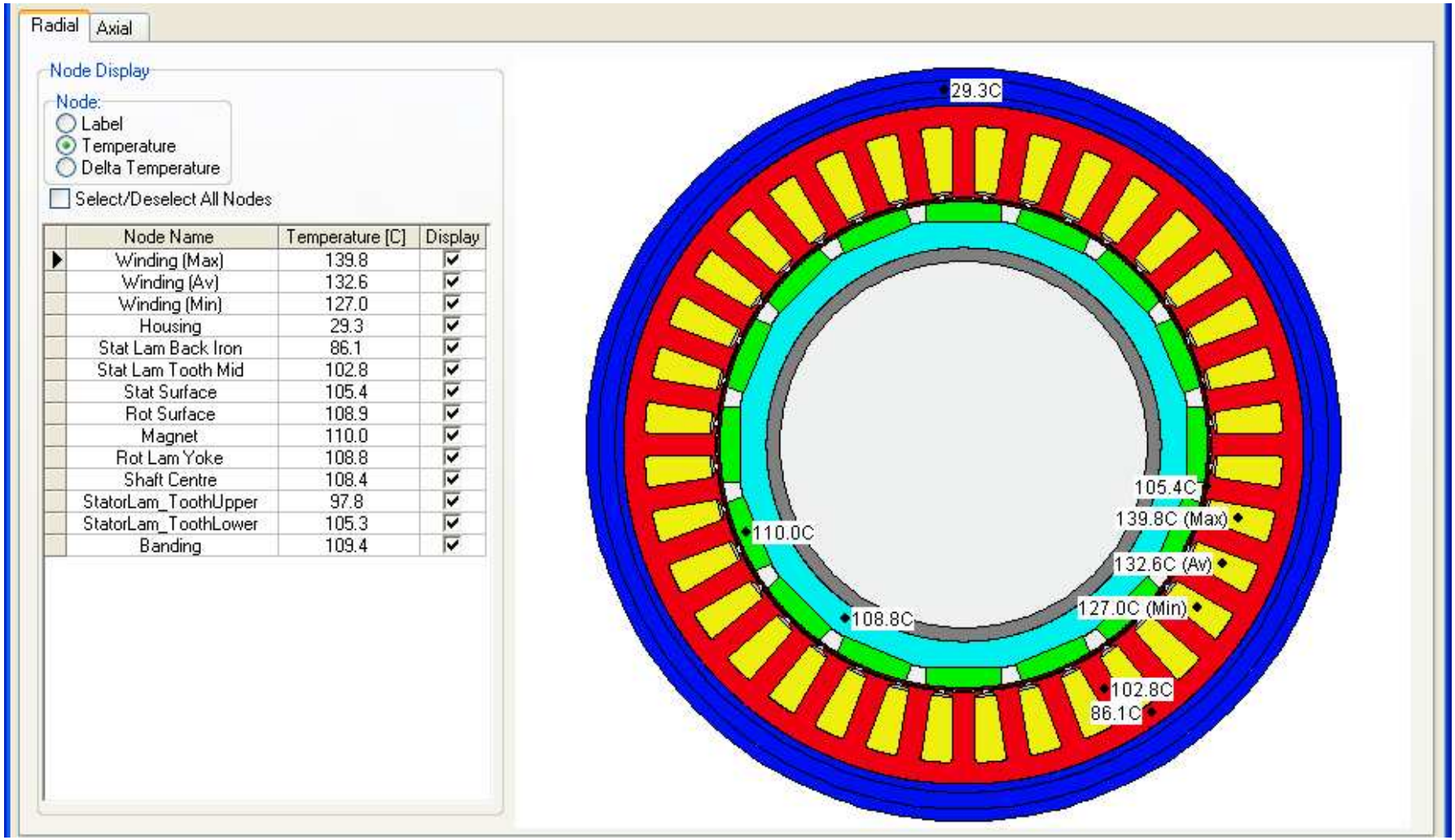

Figure 14 - Motor-CAD™ Radial Output

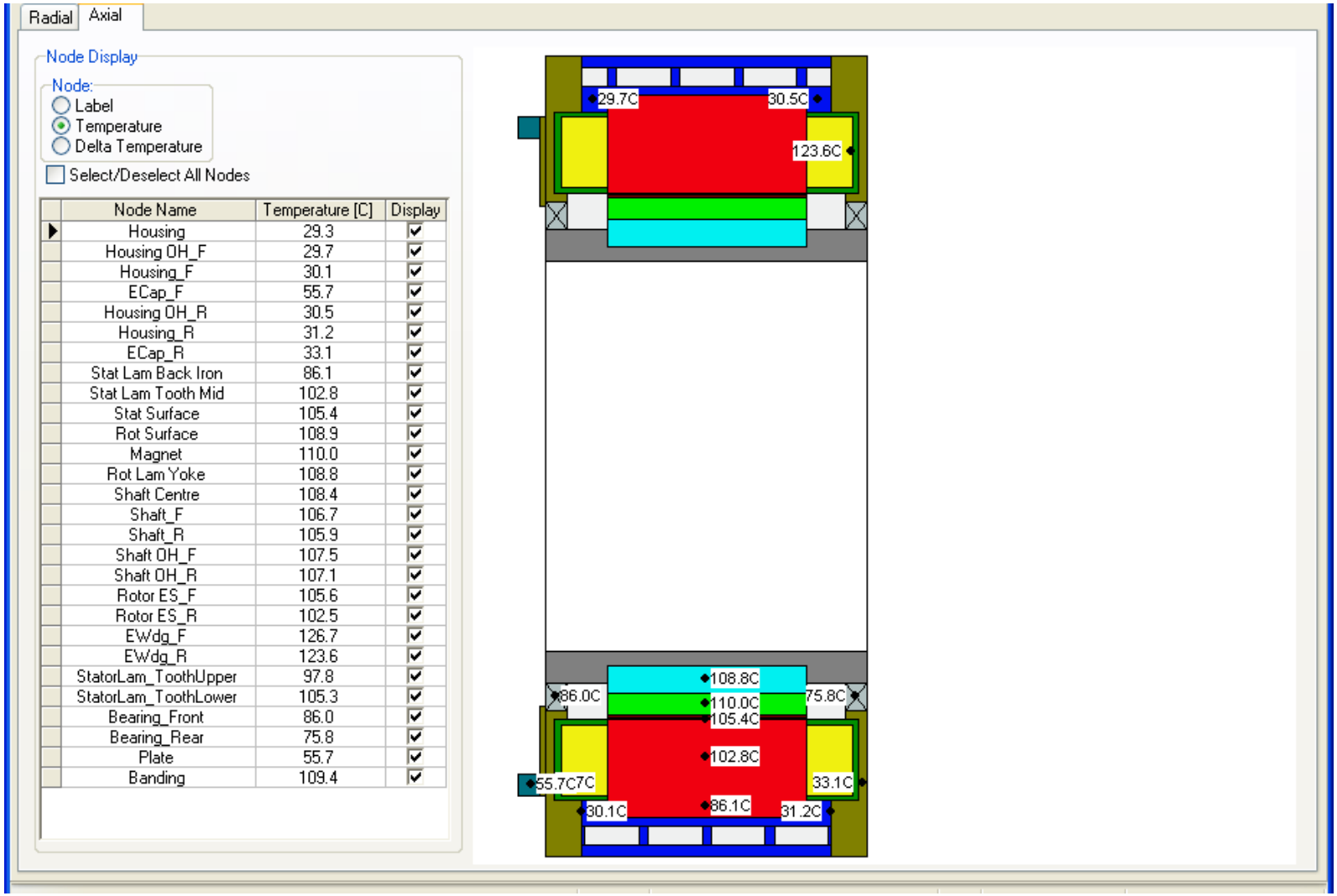

Node Name	Temperature [C]	Display
Housing	29.3	☑
Housing OH_F	29.7	☑
Housing_F	30.1	☑
ECap_F	55.7	☑
Housing OH_R	30.5	☑
Housing_R	31.2	☑
ECap_R	33.1	☑
Stat Lam Back Iron	86.1	☑
Stat Lam Tooth Mid	102.8	☑
Stat Surface	105.4	☑
Rot Surface	108.9	☑
Magnet	110.0	☑
Rot Lam Yoke	108.8	☑
Shaft Centre	108.4	☑
Shaft_F	106.7	☑
Shaft_R	105.9	☑
Shaft OH_F	107.5	☑
Shaft OH_R	107.1	☑
Rotor ES_F	105.6	☑
Rotor ES_R	102.5	☑
EWdg_F	126.7	☑
EWdg_R	123.6	☑
StatorLam_ToothUpper	97.8	☑
StatorLam_ToothLower	105.3	☑
Bearing_Front	86.0	☑
Bearing_Rear	75.8	☑
Plate	55.7	☑
Banding	109.4	☑

Figure 15 - Motor-CAD™ Axial Output

There are other features included in Motor-CAD™ that contribute to the convenient use of the software. There is an extensive materials database, including air and liquid coolant properties. The inputs surrounding air and liquid cooling are straightforward, and automatically calculate if the flow is laminar, turbulent, or borderline. The circuit editor allows for some customization of the motor geometry outside of the standard geometry, such as setting nodes to a fixed temperature. The ability to run a sensitivity analysis is another very useful tool within Motor-CAD™. Sample sensitivity analysis is shown in Section 3.4.

Motor-CAD™ is designed around commercial motors, with conventional cooling methods. The majority of help topic examples and Motor-CAD™ documentation indicate that setup and confirmation of the thermal models was performed on air-cooled, industrial motors. Liquid cooling exists as an integrated feature in Motor-CAD™, however the details and options surrounding this cooling path are not as developed as the air-cooled options, such as through ventilation. With liquid cooling, almost all of the heat is transferred though the core / housing interface and the end winding / housing interface, making these critical features in the model geometry.

One area of model predictions that does not match test data is the end winding versus slot center temperature. Utilizing Motor-CAD™, the end winding temperature is very close to the slot winding temperature, while in physical testing of high power water cooled motors the end winding temperature can be 20°C to 30°C higher than the slot center temperatures. This difference can be explained through a resistance value that is too low as shown in Figure 16. The resistance between the end winding and the slot center is calculated in Motor-CAD™ taking the thermal resistance of the copper, and one

fourth of the total end winding length. The issue with this method of calculation is that it does not include the copper resistance of the copper in the stack length. This can be worked around by using the end winding to active winding resistance modifier in the "seldom used" input section as shown in Figure 17. This multiplier should be a value of:

End Winding to Active Winding Resistance Multiplier =

[(End_Winding + 2*Stack_Length)/End_Winding].

[Eq. 1]

The end winding to active winding resistance multiplier issue has been corrected since this research has been completed, with version 5.4.7.1 of Motor-CAD™. This latest version of Motor-CAD™ includes the ability to incorporate multiple axial planes within the nodal model, incorporating the stack length resistance.

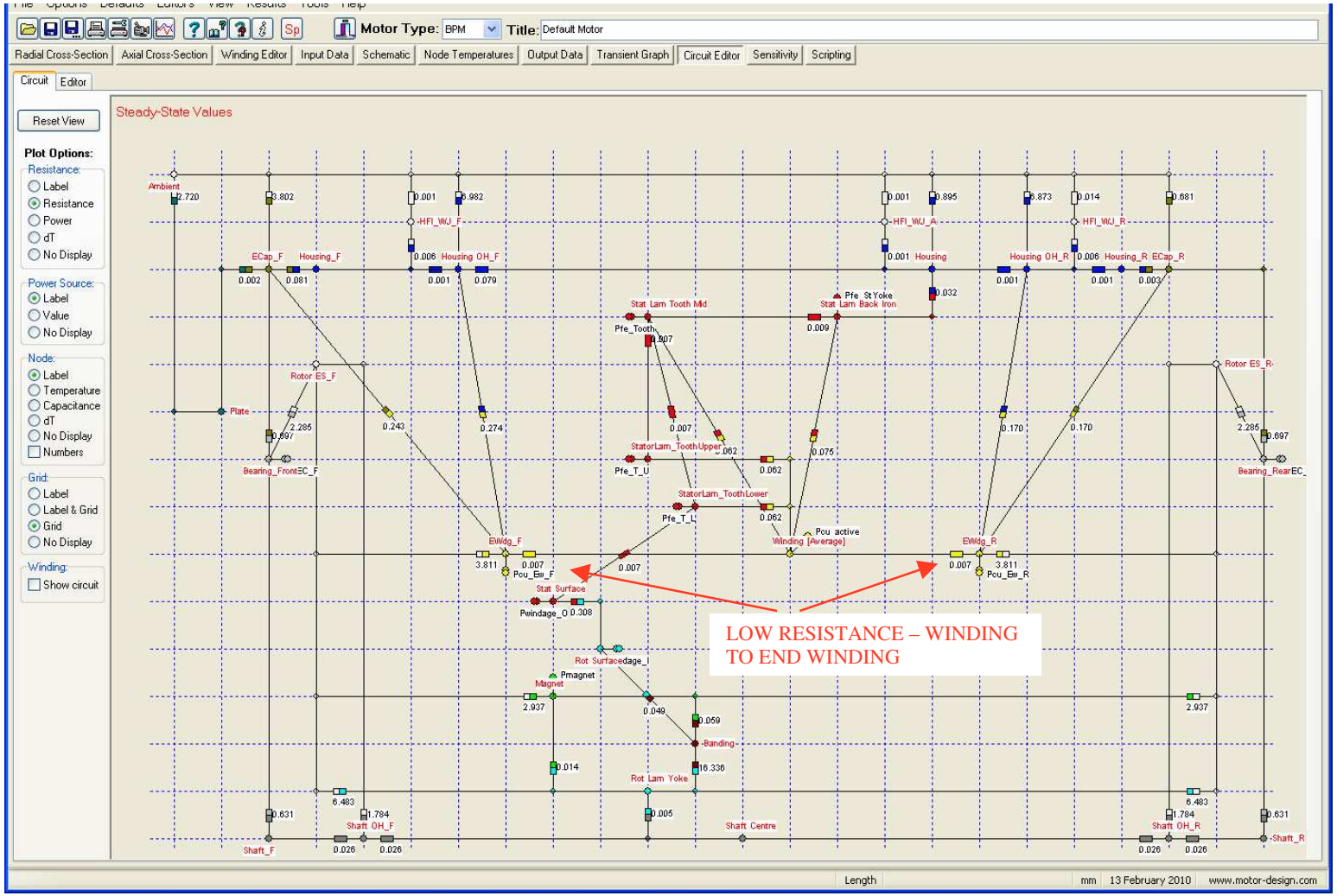

Figure 16 - Low Winding to End Winding Resistance

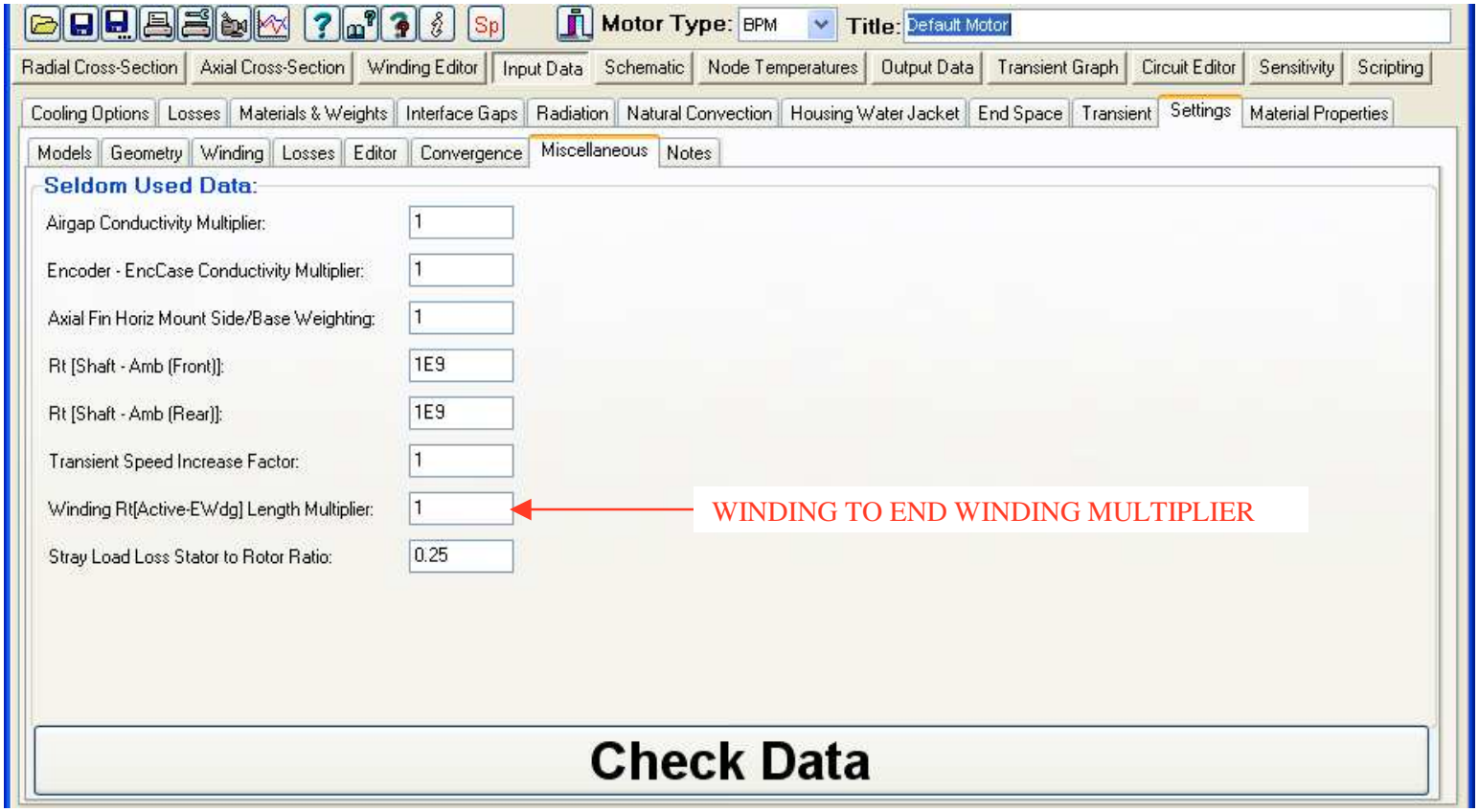

Figure 17 - Winding to End Winding Resistance Multiplier

The changing nature of heat distribution during a steady state analysis is not considered within the operation of Motor-CAD™. An example of this is the heat distribution between the end windings and active windings. As the end winding temperature increases relative to the active winding temperature the relative resistance in the end winding increases due to the physical properties of copper due to temperature. Due to the increase in relative end winding resistance, the heat distribution percentage in the end windings should increase, however the balance remains static. The work-around for this problem is to manually iterate the addition of power at the end winding nodes on the power loss sheet, as shown in Figure 18.

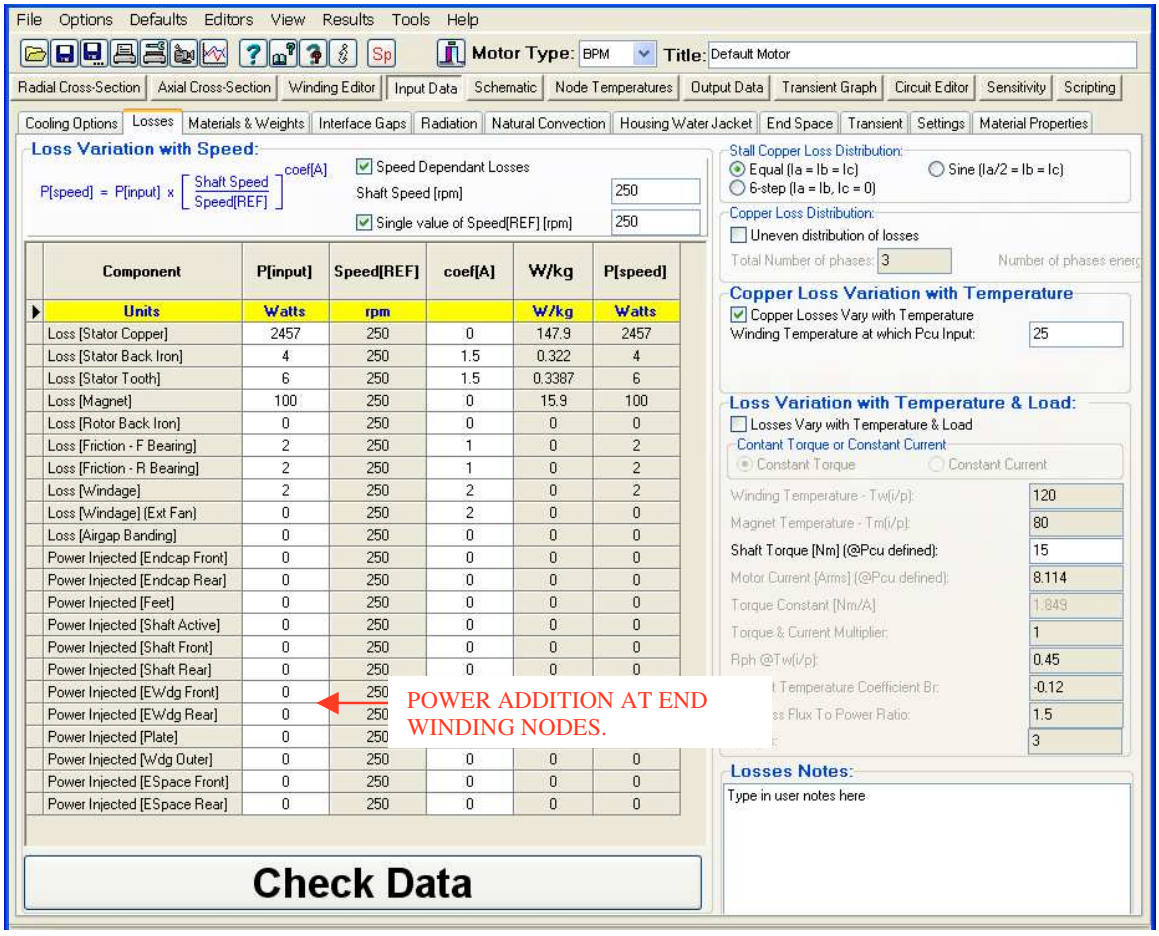

Figure 18 - Power Addition at End Windings

The resistance between the slot center and laminations is a series of resistances, as discussed in [3]. This resistance does not account for phase-to-phase slot insulation, which can be a significant thermal resistance with two or three layers of fiberglass tape. The phase-to-phase slot insulation likely adds hot spots to a motor, however it is very difficult to accurately place thermocouples in an encapsulated motor to measure the full effect of phase-to-phase insulation. This difficulty is discussed further in Section 4.1, Test Setup.

The inability to verify or modify the equations used for each resistance reduces the confidence in the thermal network. The closed nature of this commercially developed software also limits the customizability of Motor-CAD™ as it is not possible to edit the assumptions made in the equations used. These drawbacks are outweighed by the positive benefits when compared to Thermsim, including the additional modeling features in both motor and cooling type, the graphical interface, and continuous improvement updates from the manufacturer. Motor-CAD™ is recommended over Thermsim as the tool moving forward for motor thermal modeling.

3.4 Sensitivity Analysis

Motor-CAD™ includes the useful feature of being able to quickly run a sensitivity analysis. This analysis will vary single or multiple parameters and graph the results against an output of motor temperature. A sensitivity analysis was run against the Motor-CAD™ Goodness Factors, the encapsulation thermal conductivity, and the housing to core gap.

The End Winding Potting Goodness is a factor to adjust for the effectiveness of the encapsulation around the end windings. Voids, phase insulation tape, and contact gaps can all affect this factor. Due to these physical unknowns, the End Winding Potting Goodness is utilized as a correlation factor to minimize error against tested data. When evaluating the effectiveness of the correlation, the average tested values of each end winding, and the active winding outer diameter and inner diameter are utilized. The End Winding Potting Goodness is a critical factor for this sensitivity study, with average winding temperature changing from approximately 100°C to 220°C with a change in the end winding potting goodness factor from 1.0 to 0.1. The motor model correlates well to test data with a factor of 0.5. This correlation also holds true for similarly sized motors that have been tested and is illustrated in Figure 19.

Impregnation Goodness is not a critical factor for average winding temperature, with temperatures changing from approximately 100°C to 119°C with a change in the impregnation goodness factor from 1.0 to 0.1. Impregnation goodness is also utilizes as a correlation factor for this model. This motor, as well as similarly sized tested motors, correlates well to test data with a factor of 0.5. This is illustrated in Figure 20.

Encapsulation Conductivity is a strong factor, with average winding temperatures changing from approximately 110°C to 180° with a change in encapsulation conductivity from 1.5 W/m/°C to 0.5 W/m/°C. The range selected indicates a large variance in thermal conductivity for encapsulants. This sensitivity is illustrated in Figure 21.

The Stator Lam to Housing Gap is a strong factor, with average winding temperatures changing from approximately 88°C to 153°C with a change in gap from 0.00 mm to 0.20 mm. The 0.20 mm [0.008 in.] is a large radial gap. This is illustrated in Figure 22.

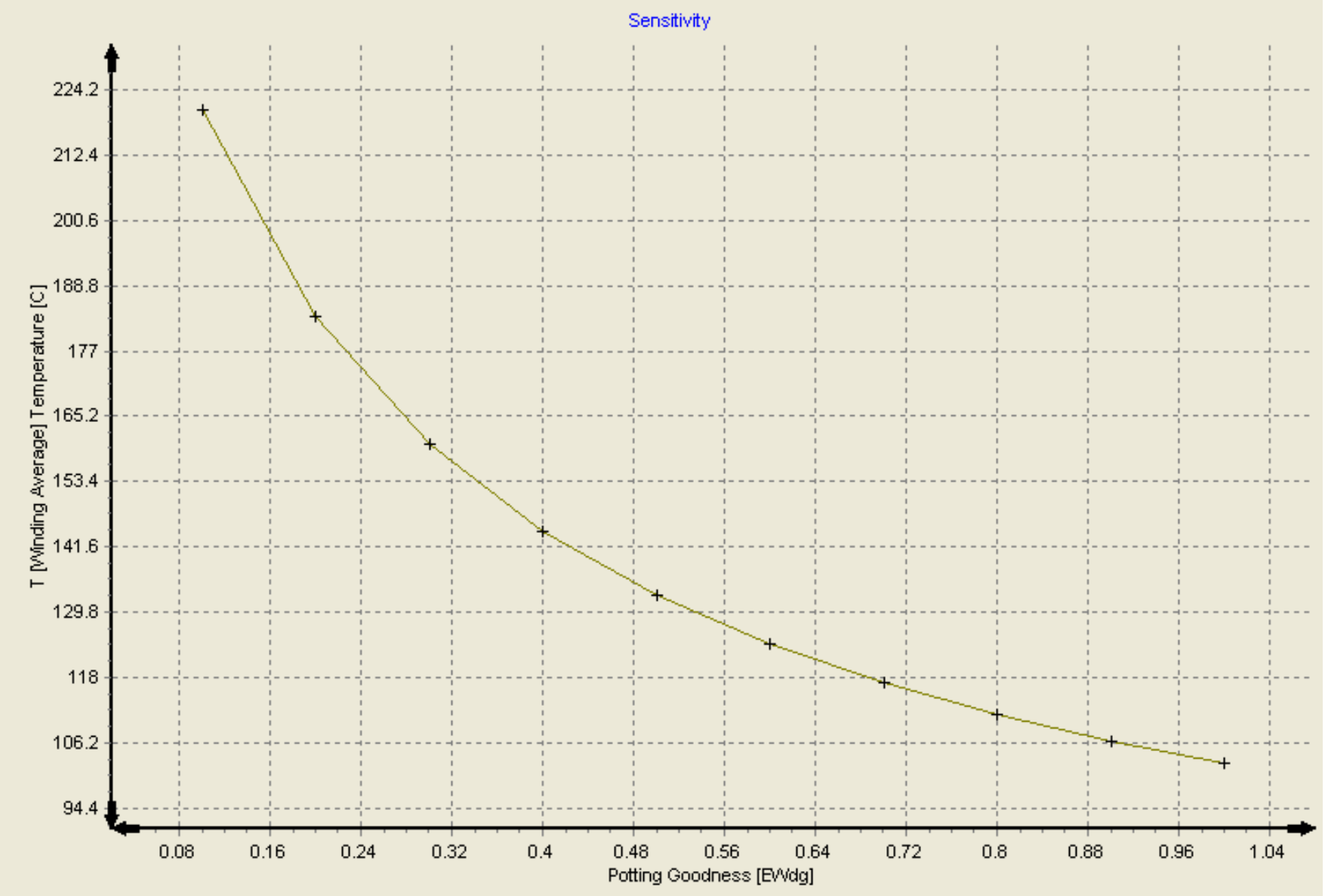

Figure 19 - End Winding Potting Goodness Sensitivity

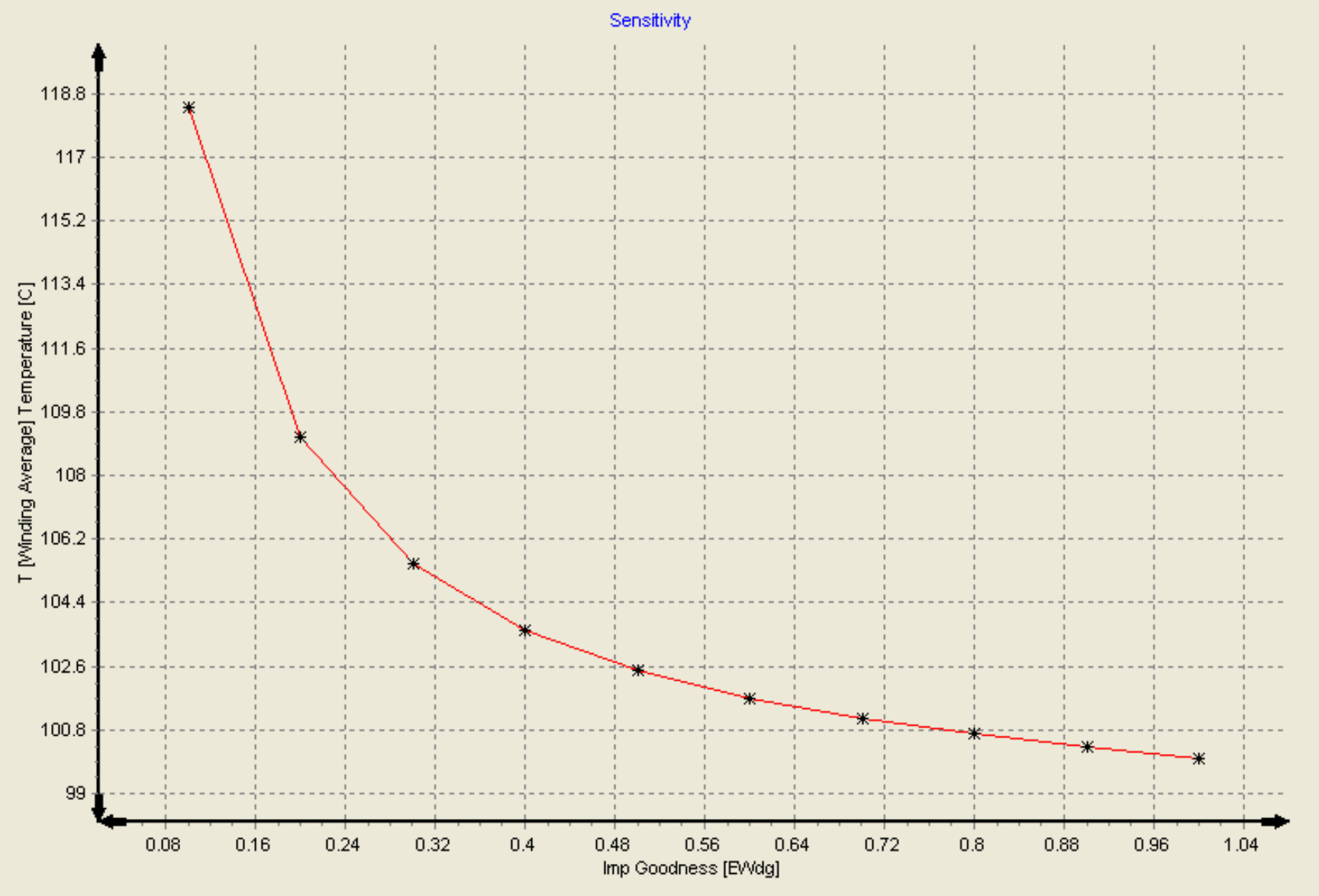

Figure 20 - Impregnation Goodness Sensitivity

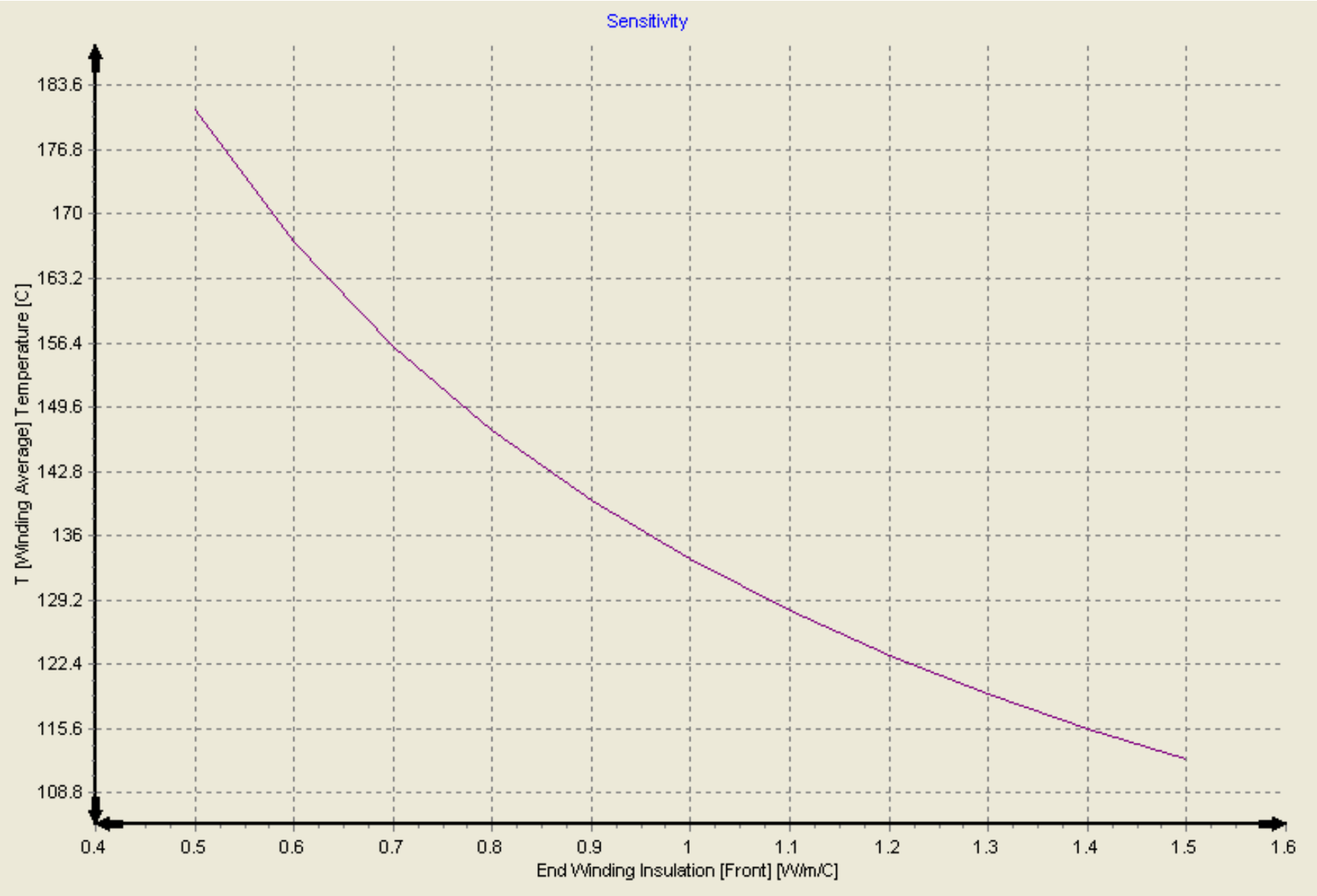

Figure 21 - Encapsulation Thermal Conductivity Sensitivity

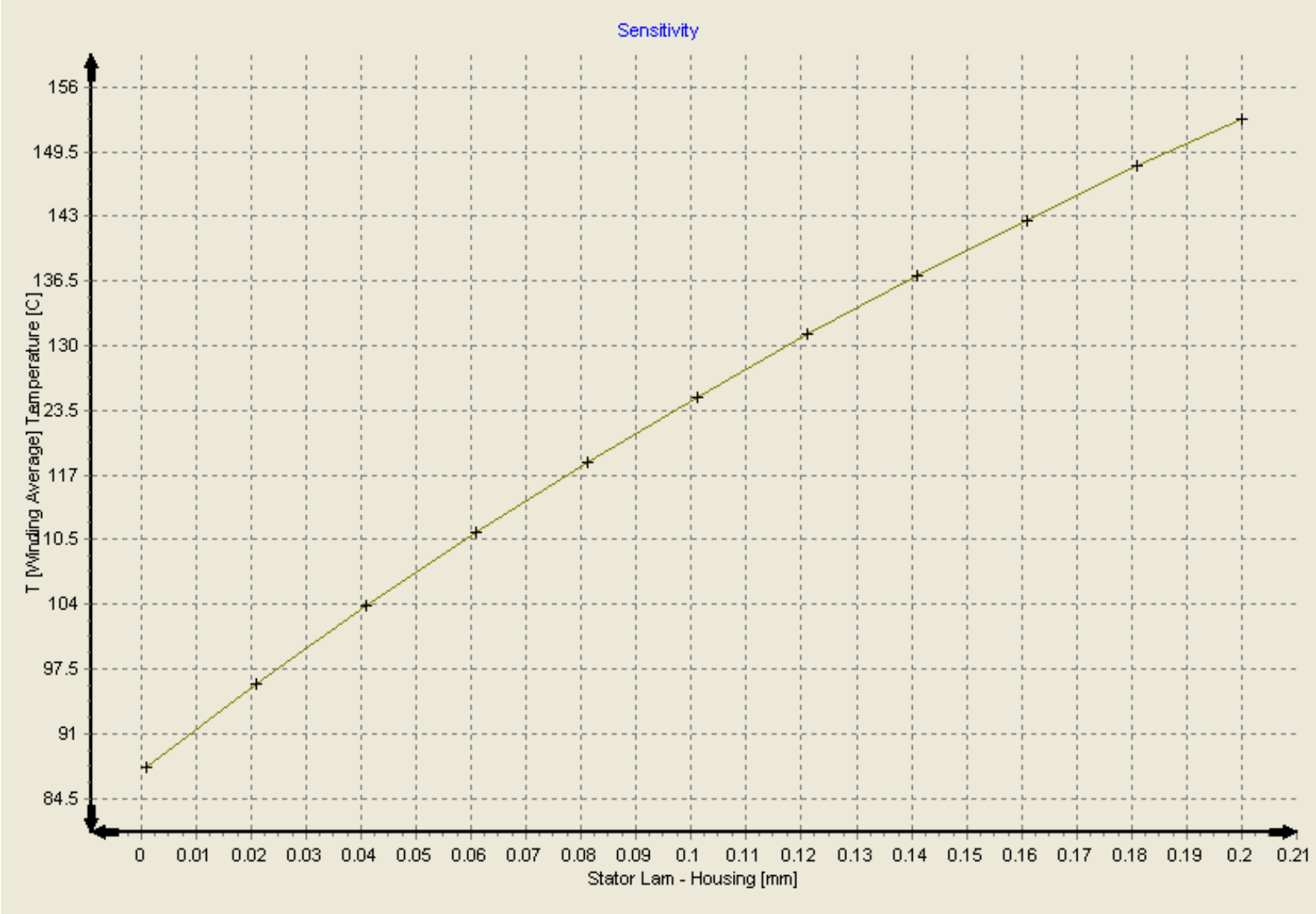

Figure 22 - Stator Lamination to Housing Gap Sensitivity

4.0 Motor Thermal Testing

4.1 Test Setup

Motor testing was performed at an outside facility driven against a load motor. The setup is such that the test motor is connected to a motor controller, while the dynamometer motor (load motor) is connected to a separate motor controller to provide the needed motor resistance for testing. The dynamometer motor functions as a generator when utilized as a resistance load for testing. An example image of a motor on a test stand is shown in Figure 23 below.

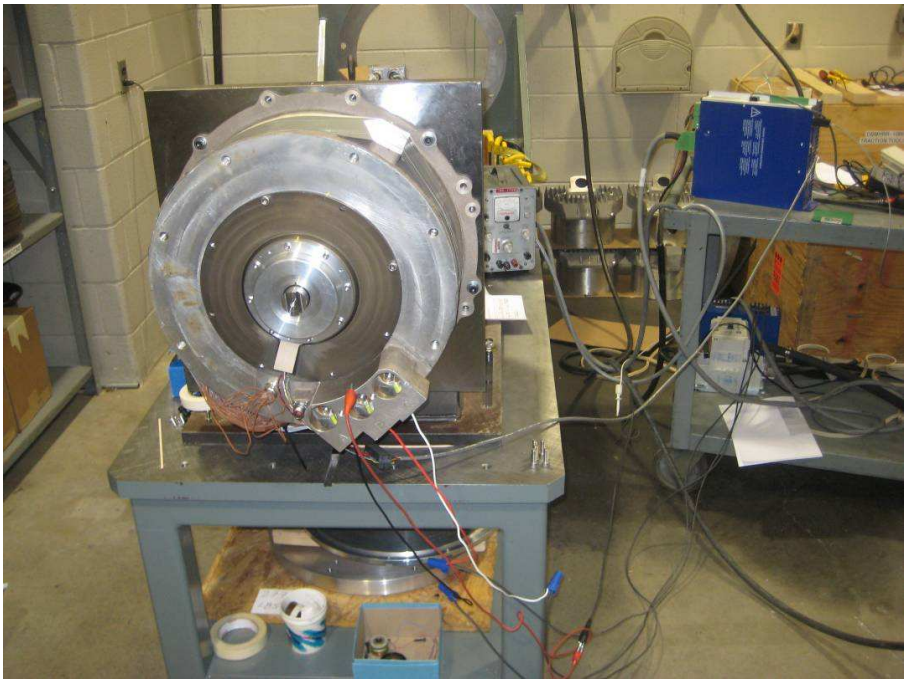

Figure 23 - Motor Mounted to Test Stand

The purpose of this testing is to provide thermal characteristics of the motor while the motor is under a prescribed load. The key evaluation criterion in motor thermal testing is thermal conductivity in units of watts lost per temperature rise. This evaluation criterion simplifies comparison testing of motors under different loads and coolant temperatures.

Motor testing was completed at full torque, 250 RPM for consistency. This is to eliminate speed-related losses that are unrelated to the thermal performance of the motor.

Test Equiptment:

Dynamometer: Outside test facility

Chiller: 50 liter per minute flow of water at 25°C and 85°C

Data analyzer: Measures test current and voltage utilizing sensors on the output cables.

Torque Transducer: 10,000 in-lbs maximum capacity, also measures RPM.

Data Logger: Multiple channel input recording power / voltage / torque and thermocouple data.

Thermocouples: Type J.

4.2 Thermocouple Placement

One of the more challenging aspects of the test setup is the determination of the thermocouple location. The thermocouples for the center of the stack length have been placed at either the ID of the motor, closest to the air gap between the insulation and the slot wedge, or at the OD of the winding slot, closest to the back iron. The ID placed thermocouples are illustrated in Figure 24, and the external placed thermocouples are illustrated in Figure 25.

Figure 24 - Internal Thermocouple Placement

The view in Figure 24 is of the ID of a motor armature looking directly at the motor teeth. The thermocouples are running down the armature between the slot liner insulation and the slot wedge designed to keep the motor winding in place.

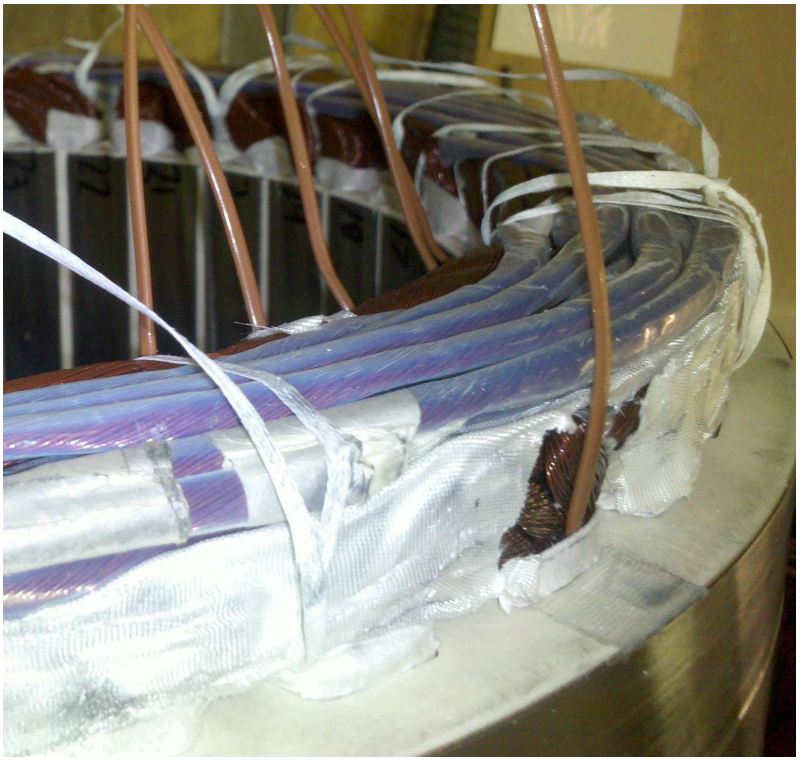

Figure 25 - External Thermocouple Placement

The view in Figure 25 is of the motor end winding showing the ID thermocouples from Figure 24 plus an additional thermocouple to capture the OD temperature of the copper winding. The copper winding filling the slot makes it impractical to place a thermocouple at the center of the winding opening, where the peak temperature will occur. The thermocouple placement limitation can account for error of up to 20°C. Figure 26 illustrates a modeled temperature variation between slot layers ranging from 123.3°C to 136.0°C, while the difference can be greater in actual test data.

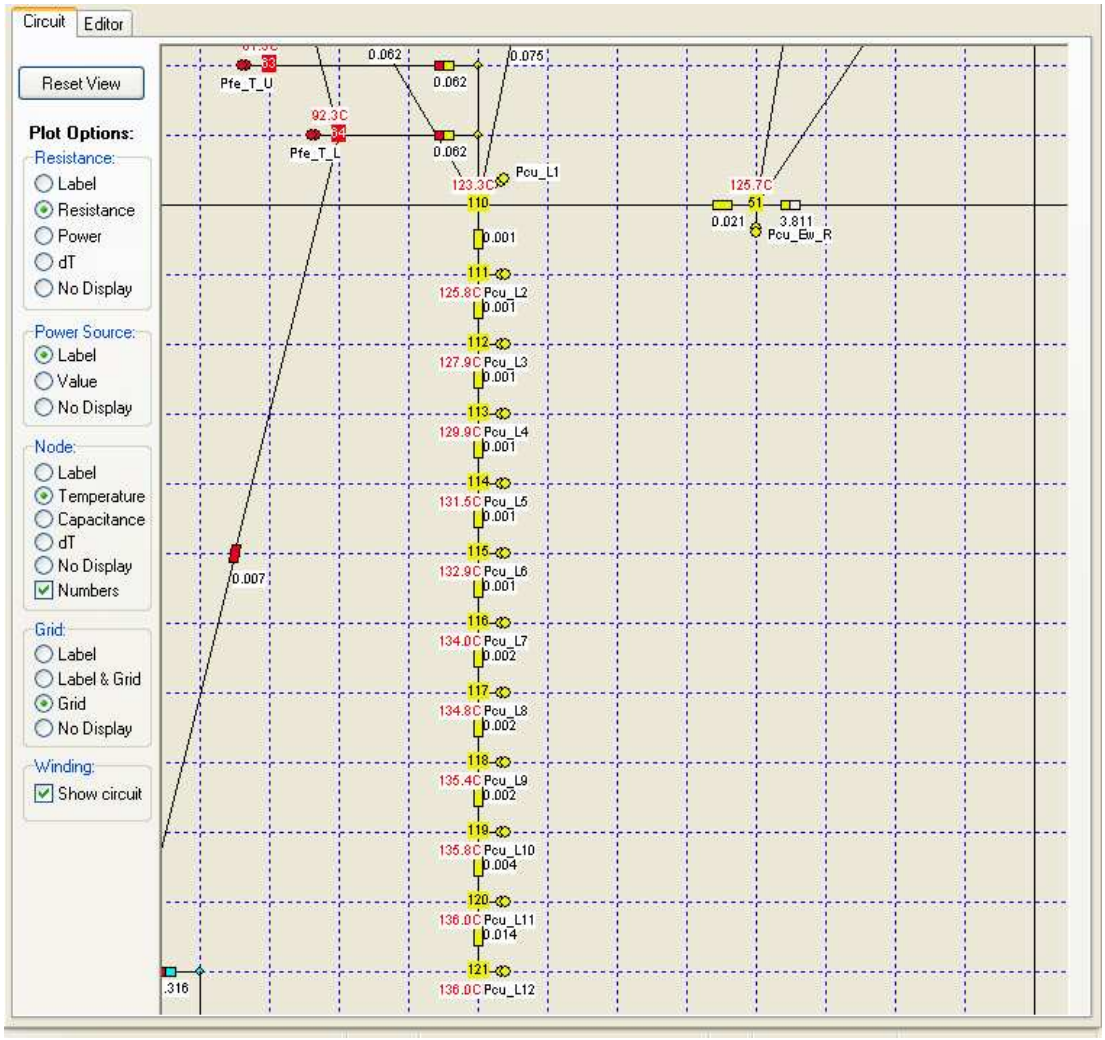

Figure 26 - Slot Temperature Variation

The end winding thermocouple placement also has significant variation. Phase insulation tape is required for these high voltage motors. This phase insulation causes thermal variations within the end windings, as well as thermal resistance variations for the thermocouples to the end-turns. As with the slot center, it is impractical to place a thermocouple directly within the center of an end winding. An illustration of the end winding thermocouple placement is shown in Figure 27.

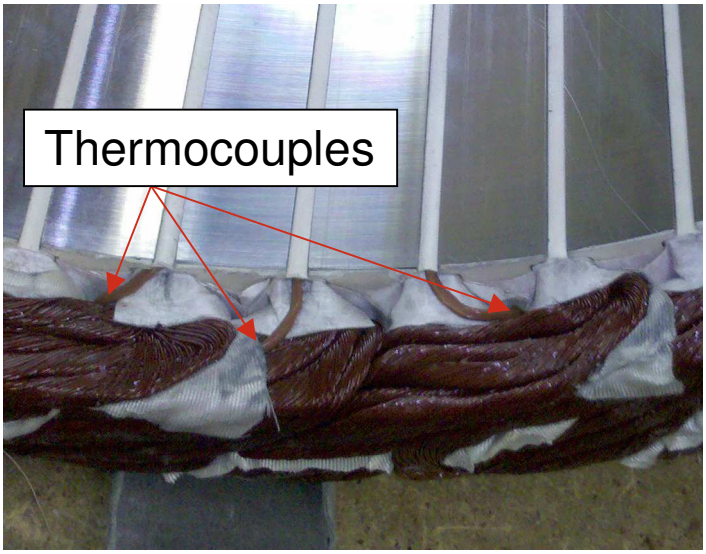

Figure 27 - End Winding Thermocouple Placement

Measured variations in end winding temperature are shown in Figure 28. Due to this variation it is unknown whether the peak hot spot of the motor has been captured during testing.

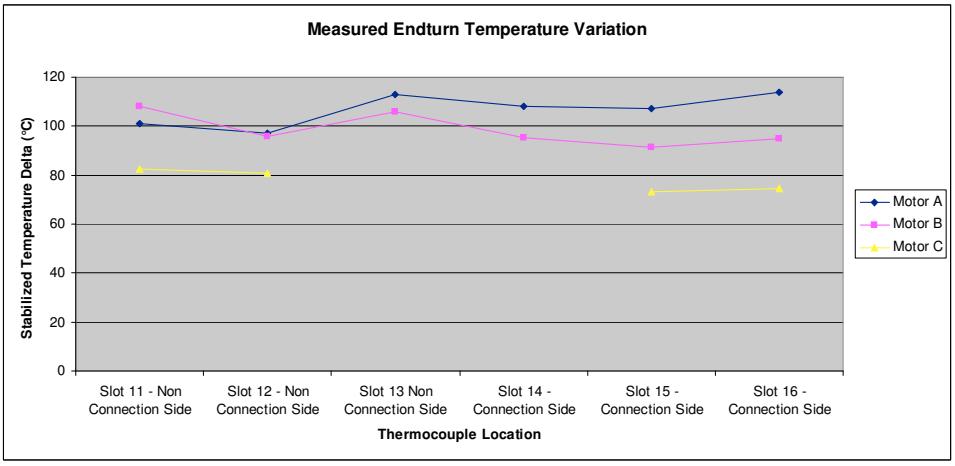

Figure 28 - Endturn Temperature Variation (250 RPM)

4.3 Baseline Motor Testing Results – Motor A

Table 1- Motor A Tested Results

Test Conditions:		
Torque	678 Nm	
Speed	250 RPM	
Copper Losses (I^2R)	4350 Watts	
Test Results:		
	Temp	Temp Rise
Connection Side End Winding	134.7 °C	109.7 °C
Opposite Side End Winding	128.7 °C	103.7 °C
Mid Stack - ID	98.6 °C	73.6 °C
Mid Stack - OD	110.7 °C	85.7 °C
	Average	Peak
Watts per temperature rise	**46.7 W/°C**	**38.2 W/°C**

The measured temperatures in the data above are averages of multiple thermocouples at the given locations. Motor testing was performed with 25°C water running through the motor housing at approximately 30 liters / minute. When evaluated as watts per temperature rise, this motor has a value of 46.7 Watts / °C temperature rise on average and 38.2 Watts / °C peak motor temperature rise.

The measured Watts per temperature rise value for this motor requires improvement in order to meet performance and package size requirements of a vehicle application. A larger value of Watts per temperature rise indicates a thermal improvement as more losses can be dissipated through the motor cooling section.

4.4 Motor Improvements and Nomenclature

Based upon the thermal modeling and the modifiable variables, improvements in motor encapsulation were evaluated in order to obtain improved motor thermal characteristics. The improvements in encapsulation were tested in two different motor iterations against the baseline motor. For clarity, the following naming convention is used to refer to the different tested motors:

Motor A – Baseline Motor

Motor B – First set of improvements, including improved encapsulation

Motor C – Second set of improvements, including improved encapsulation with reduced voids.

4.5 Encapsulant Improvements Formulation and Testing

The improved encapsulant was developed specifically to have a high thermal conductivity coupled with high electrical resistance. The encapsulant was also formulated to withstand temperatures upwards of 200°C, increasing the typical temperature rise allowed in a motor. Development of this encapsulant was optimized through small sample material testing, followed by small sample motor builds. Papers discussing high conductivity encapsulations are shown in [10-14], however the encapsulations discussed are either not commercially available or not appropriate for a high temperature engine environment.

Material testing of the encapsulant was initially performed by comparison to known encapsulants. This allowed the testing to be performed quickly, in house, and without the additional expense of sending many samples to a test lab. The testing involved placing identically sized samples on a large heated mass, and comparing the time difference for the top surfaces to heat up. This setup is illustrated in Figure 29 - Rapid Comparison Test Setup. This method does not provide an exact measure of thermal conductivity, however this comparison does provide a good estimate, allowing the optimum mixture to be quickly tested.

The optimum encapsulant mixture as developed in the pure material state required modification in order to properly fill a motor with a high copper to encapsulant ratio without voids. This experimentation was performed on smaller motors, and later verified with larger motor productions. This resulted in a mixture that did not have the highest

thermal conductivity, however when coupled with improved fill and reduced voids the mixture produced the best thermal solution for the motor.

Figure 29 - Rapid Comparison Test Setup

4.6 Encapsulation Issues

The high copper fill of typical vehicle motors makes encapsulation difficult with thicker encapsulants required for high thermal conductivity. This is shown in Figure 30 - Slot Cross Section - Machined. This view is of a cross section of the wound motor armature, showing the laminations and motor windings. This view illustrates the tight copper bundles preventing the flow of encapsulation. In "Motor B" there were a significant number of large voids due to the viscosity of the improved encapsulant. This is evident on the inner diameter of the motor, as shown in Figure 31 and Figure 32, however there is no way to determine the severity and location of all of the motor voids without destruction of the motor.

For “Motor C”, the encapsulation formula was modified in order to significantly reduce voids. A clear reduction in voids was evident on the ID of this motor versus the first motor, however there is still some evidence of small void formation. This is shown in Figure 33. This shows that there are still a few slots that did not fill with encapsulant, but for the majority of slots, there is evidence of encapsulation going through the motor. As with the baseline motor, it is not possible to evaluate the severity or location of encapsulation voids.

Figure 30 - Slot Cross Section - Machined

Figure 31 - Ecapsulation Voids, "Motor B" Inner Diameter

Figure 32 - Encapsulation Voids, Close Up – "Motor B"

Figure 33 - "Motor C" Encapsulation Fill

4.7 Motor B Results

Table 2 - Motor B Tested Results

Test Conditions:		
Torque	723 Nm	
Speed	250 RPM	
Copper Losses (I^2R)	4722 Watts	
Test Results:		
	Temp	Temp Rise
Connection Side End Winding	118.8 °C	93.8 °C
Opposite Side End Winding	128.2 °C	103.2 °C
Mid Stack - ID	111.2 °C	86.2 °C
Mid Stack - OD	110.9 °C	85.9 °C
	Average	Peak
Watts per temperature rise	**51.2 W/°C**	**43.7 W/°C**

This motor has improved encapsulation, optimized for thermal conductivity. The thermal conductivity is estimated at 2.6 w/m² °C due to the voids present within the

encapsulant. This motor was tested with eight percent more current and therefore more thermal losses than the baseline motor. Even with this increase in thermal losses, both end winding temperatures are significantly reduced. The mid-stack OD thermocouples are relatively unchanged, while the mid-stack ID thermocouples show slight increases in temperature. This aligns well with an increase in losses coupled with an increase in thermal conductivity. The increase in thermal conductivity will have a significantly larger effect on the end winding temperature than on the ID of the slot, where a significant portion of the heat loss will go to the core teeth and ID. It is also possible that the thermocouple reads higher due to higher thermal conductivity to the adjacent winding. When evaluated as watts per temperature rise, this motor has a value of 51.2 Watts / °C temperature rise on average and 43.7 Watts / °C peak motor temperature rise. This is a thermal improvement of 9.6% on average and 14.5% peak as compared to the baseline motor.

4.7 Motor C Results

The main improvement for "Motor C" is a reformulation of the encapsulant to enhance flow and therefore achieve a reduction in voids, as discussed above. A reduction in armature adhesive was also made concurrently to reduce the contact resistance between the stator core and housing. This motor was tested at 85°C water in order to more closely simulate the vehicle application, however temperature rise data can still be utilized for comparison. These combined changes resulted in the following tested values:

Table 3 - Motor C Tested Results

Test Conditions:		
Torque	627 Nm	
Speed	250 RPM	
Copper Losses (I²R)	4785 Watts	
Test Results:		
	Temp	Temp Rise
Connection Side End Winding	159.0 °C	74.0 °C
Opposite Side End Winding	165.4 °C	80.4 °C
Mid Stack - ID	152.6 °C	67.6 °C
Mid Stack - OD	151.2 °C	66.2 °C
	Average	Peak
Watts per temperature rise	**64.8 W/°C**	**59.5 W/°C**

This motor has a clear improvement in temperature from both the baseline and improved motors. When evaluated on a Watts / temperature basis, this motor allow 64.8 Watts / °C temperature rise on average and 59.5 Watts / °C temperature rise peak. This is a 56% peak improvement and 39% average improvement in thermal capacity vs. the baseline motor.

5.0 Summary and Conclusion

5.1 Motor A Results Summary

The thermal modeling of these motors provides both an accurate picture of thermal challenges and areas that will best provide for improvement. Both of the internal and commercially available thermal software were correlated to the baseline model, and further utilized to indicate the expected improvement. The baseline "Motor A" model correlation is shown Table 4 below:

Table 4 - Motor A Results Summary

Baseline – Motor A Temperature Rise	Measured Values	Thermsim	Motor-CAD™
Connection Side Endturn	109.7℃	112.9℃	101.7℃
Opposite Side Endturn	103.7℃	121.0℃	102.4℃
Mid Stack – OD	85.7℃	107.9℃	96.4℃

The model conditions used for this baseline motor are as follows:

Stator laminations to housing gap: .002"

Encapsulant to housing gap: .010"

Encapsulant thermal conductivity: 1.01 W/m-k (commercially available)

The encapsulant to housing gap accounts for motor insulation tape that is secured around the motor end windings, while the stator lamination to housing gap accounts for the layer of adhesive securing the stator laminations in place.

The Thermsim values correlate to within 26% of the tested data, with the Mid Stack - OD of the Thermsim model showing the most variation, while the Motor-CAD™ values correlate to within 13%. This large error on the Thermsim Mid Stack – OD can be partially attributed to location mismatch between the nodal and measured temperatures. The Thermsim Mid Stack – OD temperature is an average slot temperature as this is the only available data point, while the Motor-CAD™ temperature is the minimum slot temperature, as this most closely represents the temperature at the location of the slot that measurement was available.

5.2 Motor B Results Summary

The improved "Motor B" results are shown in Table 5 below.

Table 5 - Motor B Results Summary

Motor B Temperature Rise	Measured Values	Thermsim	Motor-CAD™
Connection Side End Winding	93.8℃	91.6℃	100.7℃
Opposite Side End Winding	103.2℃	104.6℃	102.0℃
Mid Stack - OD	85.9℃	89.8℃	97.3℃

These models also show a very close correlation to the tested data. The only change from this model "B" to the baseline "Motor A" model is the adjustment of the encapsulant thermal conductivity from 1.01 W/m-k to 2.6 W/m-k, accounting for the improved formulation of motor encapsulant.

5.3 Motor C Results Summary

Table 6 - Motor C Results Summary

Motor C Temperature Rise	Measured Values	Thermsim	Motor-CAD™
Connection Side End Winding	74.0°C	75.0°C	72.7°C
Opposite Side End Winding	80.4°C	89.4°C	73.7°C
Mid Stack - OD	66.2°C	74.8°C	67.7°C

This motor "C" also has a strong correlation to the measured results. The changes to this motor include a thermal encapsulation value of 3.2 W/m-k to account for the removal of encapsulation voids, a stator lam to housing gap of .0005" as the majority of glue was removed from this joint and relocated to specialized "glue grooves", and an encapsulation to housing gap of .008" as the tape layer thickness was reduced within this motor.

5.4 Improvement Discussion

Motor thermal improvements of approximately 40% have been achieved through improvements in encapsulation and adjustments to internal motor interfaces. While there is a cost associated with the improved encapsulation, it is a relatively inexpensive solution when compared to the alternative of increasing motor size. The increase in required motor size to achieve the same performance without the thermal improvements discussed is not a direct 1:1 ratio as some losses are fixed regardless of size, such as in the end windings. The increase in size however would be close to the 40% improvement shown. This size increase would result in an increase in raw material upfront along with overall vehicle performance losses due to the added weight and packaging. These thermal improvements are a practical design feature for high performance vehicle motors.

5.5 Conclusions

The use of electric motors on vehicles requires high power in a lightweight and small package. Additional mass on a vehicle reduces fuel efficency, range, and overall vehicle performance characteristics, while a large motor packaging size is generally not available within the constraints of the vehicle size. Thermal limitations of high power vehicle motors limit the motor performance within an available motor package. Vehicle motors are typically liquid cooled in order to obtain the highest motor and vehicle performance. This research has shown significant thermal improvements to high-powered liquid cooled vehicle motors through modeling and experimentation.

Through the winding encapsulation and process improvements shown in this research, motor thermal improvements of approximately 40% were achieved, as measured Watts / °C temperature rise. Thermal improvements through encapsulation thermal conductivity increases and a reduction of thermal resistance due at the contact interface between the stator windings and liquid cooled housing were modeled using both the commercially available Motor-CAD™ software and the internally developed Thermsim thermal modeling software. Both software packages indicated a significant improvement from these thermal changes, and the Motor-CAD™ software package correlated to within 14% of the actual tested data for all three motors tested. The Thermsim software correlated to within 26% for the three motors tested, due to a mismatch between the modeled node location and thermocouple measurement location. Through this correlation, the lumped parameter thermal modeling method is shown as an accurate and cost effective method for determining thermal parameters of high power

liquid cooled motors. Motor thermal modeling is also shown to be very useful in determining effective thermal improvement techniques.

Future work could include additional thermal improvements closest to the heat source, such as reducing the thermal contact resistance between the slot liner paper insulation and the motor laminations. If thermal improvements for that interface can easily be made, it is likely that a thermal model and testing will indicate significant motor thermal improvements. Further additional work could also include continued improvements to the encapsulation system to ease manufacturing and further reduce voids within the encapsulation fill.

References

1. Boglietti, Aldo, Andrea Cavagnino, David Staton, Martin Shanel, Markus Mueller, and Carlos Mejuto, "Evolution and Modern Approaches for Thermal Analysis of Electrical Machines," *IEEE Transactions on Industrial Electronics*, Volume 56, Number 3, March 2009.

2. Motor-CAD™ Version 5.3.4.1 - http://www.motor-design.com

3. Boglietti, A., A. Cavagnino, and D. Staton, "Determination of Critical Parameters in Electrical Machine Thermal Models," *IEEE Transactions on Industry Applications*, Volume 44, Issue 4, July 2008.

4. Staton, Dave, Aldo Boglietti, and Andrea Cavagnino, "Solving the More Difficult Aspects of Electric Motor Thermal Analysis," *IEEE Transactions on Energy Conversion*, Volume 20, Number 3, September 2005.

5. Mellor, P.H., D. Roberts, and D.R. Turner, "Lumped Parameter Thermal Model for Electrical Machines of TEFC Design," *IEE Proceedings-B*, Volume 138, Number 5, September 1991.

6. Liu, Z.J., D. Howe, P.H. Mellor, and M.K. Jenkins, "Thermal Analysis of Permanent Magnet Machines," *6th Int. Conf. On Electrical Machines & Drives,* Conf. Pub No. 376, September 1993

7. Ayman, M., Nathan C. Harris, Thomas M. Jahns, and Khwaja M. Rahman, "Thermal Analysis of Multibarrier Interior PM Synchronous Machine Using Lumped Parameter Model," *IEEE Transactions on Energy Conversion*, Volume 19, Number 2, June 2004.

8. Gerling, Dieter and Gurakuq Dajaku, "Novel Lumped-Parameter Thermal Model for Electrical Systems," *European Conference on Power Electronics and Applications,* Dresden, Germany, 2005.

9. Dajaku, G. and D. Gerling, "An Improved Lumped Parameter Thermal Model for Electrical Machines," *Proceedings of the 17th International Conference on Electrical Machines (ICEM),* Chania, Greece, 2006.

10. Neal, G.D., O. Kwon, and D.K. Lieu, "Ceramic Filled Thermoplastic Encapsulation as a Design Feature for a BLDC Motor in a Disk Drive," *IEEE Transactions on Magnetics*, Volume 37, Issue 2, March 2001.

11. Wong, C.P. and Raja S. Bollampally, "Comparative Study of Thermally Conductive Fillers for Use in Liquid Encapsulants for Electronic Packaging," *IEEE Transactions on Advanced Packaging*, Volume 22, Number 1, February 1999.

12. Han, Z., J.W. Wood, H. Herman, C. Zhang, and G.C. Stevens, “Thermal Properties of Composites Filled with Different Fillers,” *Conference Record of the 2008 IEEE International Symposium on Electrical Insulation,* Vancouver, BC, June 2008.

13. Miller, M.L. and F. T. Emery, “Thermal Conductivity of High Voltage Stator Coil Groundwall Insulation,” *Electrical Insulation Conference Proceedings*, Rosemont, IL, September 1997.

14. Neal, Griffith D. and James M. Finan, “Thermally Conductive Thermoplastics-A Viable Alternative for Coil Wound Device and Passive Component Construction,” *Electrical Insulation Conference Proceedings*, Cincinnati, OH, October 1999.

Appendix A - Thermsim Excel Input

Thermsim version 4.6.4
E.Filip
18-Mar-09

Application: **FILL ME IN**
to be used with simulink file: **Thermsim_464**

1. Enter Data Here (only in yellow cells)

	units: mm, Nm	Inputs (inch):	options:
stator housing	stator housing or endcaps (like RBEH)		housing or endcap
	if endcap, enter distance endbell overlaps stator		
	housing material		aluminum, steel, stainless
	OD housing		
	ID housing over front end turn		
	ID housing over rear end turn		
	motor length, total		
	distance rear endturn to rear endbell		
	distance front endturn to front endbell		
	rear ecap in contact with endbell?		y or n
	rear ecap in contact with housing?		y or n
	front ecap in contact with endbell?		y or n
	front ecap in contact with housing?		y or n
	Fin Multiplier		
front endbell	material, front endbell		aluminum, steel, stainless
	thickness, front endbell		
	Is the housing and FEB 1 piece?		y or n
	Is the housing and REB 1 piece?		y or n
rear endbell	material, rear endbell		aluminum, steel, stainless
	thickness, rear end bell		
brake heat	brake heat (watts)		
mount	material, mounting surface		aluminum, steel, stainless, ti
	OD of mounting surface		
	thickness mounting surface		
	Fixed mounting temp (C°) - leave blank if not **fixed**		
front shaft seal	friction torque (ozin)		
front bearing	OD front bearing		
	front bearing friction torque (ozin)		
rear bearing	OD rear bearing		
	rear bearing friction torque (ozin)		
magnet	material		neo, sam
	weight (lb)		
	length (WMM)		
	face width (HME)		
	diameter of magnet seats (DMC)		
field	material, field		steel only for now

Thermsim Excel Input Page - Part 1

shaft		material, shaft		steel only for now
		diameter, between field and front bearing		
		diameter, between field and rear bearing		
IS SHAFT EXPOSED TO OUTSIDE AIR?		length, shaft		
(Y or N)	**N**	inside diameter		
		additional surface area exposed to outside air		
stator lam		ID aramture (IDA)		
		OD stator lam		
		Tooth Volume (VT)		
		Core Volume (VC)		
		stack length (WA)		
		number slots (S)		
		slot width at bottom (WSB)		
		slot winding area (SWA)(in^2)		
		slot bottom diameter (DSB)		
		length of tooth (LT)		
		lam edge radius (in)		
		lam thickness (in)		
stator assy		front endturn length (in)		
		rear endturn length (in)		
		endturn OD (in)		
		MLT mean length of turn (ft)		
other		air gap (GAP)		
		wire gage (AWG)		
		slot liner material		kapton, fluidize
		slot liner thickness		
		slot fill factor		
		endturn insulation		IM461, IM436, IM21880, varnish
		varnish thickness (in)		
		armature / housing press fit		press, slip
		armature / housing radial gap (in)		
		arm / hsg epoxy coverage ratio		%
		pressure of fit, armature/ housing		
cooling method		water or air		forced water, air
		cooling air velocity (ft/sec)		
		water flow rate (gal / min)		
		cooling fluid		water, glycol, oil Mobil shc 624, oil Mobil shc 630
		Number of parallel stator cooling tubes		
		pipe hydraulic diameter		
		pipe length per stator coolant channel		
		Stator coolant temp (deg C)		
		ambient air temperature (deg C)		
		initial temperature (deg C)		
		estimated housing temperature (deg C)		
Rotor		rotor cooling?		yes, no
		End Ring Surface Area (mm^2)		mm^2
		End Ring Surface Avg Speed (m/s)		m/s
		rotor coolant flow rate (gpm)		
		rotor coolant		oil 624, oil 630, air
		rotor cooling tube diameter (in)		
		rotor tube length (in)		
		rotor tube surface area (in^2)		
		Number of parallel rotor cooling tubes		
		Diameter (BC) of cooling tubes		
		rotor endring cooling tube diameter		
		rotor end ring tube length (per endring)		
		rotor endring tube surface area (in^2)		
		Rotor coolant inlet temp(deg C)		
		rotor press fit pressure		
		axial thickness of flow region		
		rotor conductor		aluminum, copper
		rotor slot width		
		rotor slot height		
		number of rotor slots		
		endring length		
		endring ID		
		endring OD		
		assumed rotor temp (deg C)		
		rotor coolant on endturns		yes, no
Motor Performance Parameters		Rm (ohms @ 20℃)		
		Kt (ozin/amp DC)		
		Tf (ozin)		

Thermsim Excel Input Page - Part 2